Earth-Science Reviews 238 (2023) 104341

Contents lists available at ScienceDirect

Earth-Science Reviews

journal homepage: www.elsevier.com/locate/earscirev

Biogeodynamics of Cretaceous marine carbonate production

Thomas Steuber [a,*], Hannes Löser [b], Joerg Mutterlose [c], Mariano Parente [d]

[a] Khalifa University of Science and Technology, Earth Sciences Department, PO Box 127788, Abu Dhabi, United Arab Emirates
[b] Universidad Nacional Autónoma de México, Instituto de Geología, Estación Regional del Noroeste, Hermosillo, Sonora, Mexico
[c] Ruhr Universität Bochum, Institut für Geologie, Mineralogie und Geophysik, 44780 Bochum, Germany
[d] Università di Napoli Federico II, Dipartimento di Scienze della Terra, dell'Ambiente e delle Risorse, Napoli, Italy

ARTICLE INFO

Keywords:
Plankton
Benthos
Calcite
Aragonite
Environment
Diversity

ABSTRACT

We have compiled stratigraphic ranges of genera of calcareous nannofossils, calcispheres, planktonic foraminifers, larger benthic foraminifers, corals and rudists bivalves, and species of dasycladalean green algae. These taxa comprise the main planktonic and benthic carbonate producers of the Cretaceous, a period of exceptionally high sea level and palaeotemperatures that was characterized by unique assemblages of benthic carbonate producers and the significant rise in pelagic carbonate sedimentation. The autecology, physiological control on calcification, and carbonate-production potential of these groups is summarized. The observed diversity patterns are compared with proxy data of Cretaceous climate and seawater chemistry to elucidate the effect of environmental change on carbonate production and sedimentation.

Two characteristic patterns are recognized. Diversity of calcareous nannofossils, calcispheres, planktonic foraminifers and corals trace the evolution of Cretaceous sea-level, while the diversity of dasycladalean algae, larger benthic foraminifers, corals and rudist bivalves show significant reductions at the level of oceanic anoxic events (OAEs). Benthic carbonate producers except for corals thus appear to have been more vulnerable to environmental change, and these general patterns appear to be unrelated to the autecology of the taxa investigated. The expansion of suitable habitats during episodes of high sea level and high temperatures appears to have been a more important control of diversity in calcareous nannofossils, planktonic foraminifers, and corals than changes in seawater chemistry. Aragonitic or aragonite-dominated benthic carbonate producers are most affected during extinction events related to OAEs, and there is a general trend of decreasing aragonite dominance throughout the Cretaceous. This is compensated by the extensive formation of calcitic hemipelagic chalk since the Cenomanian. The trend of decreasing aragonite dominance is independent of the level of biological control on calcification in the different taxa affected. The demise of aragonitic or aragonite-dominated carbonate producers at OAE1a (early Aptian) and OAE2 (Cenomanian–Turonian boundary interval) may be related to short episodes of reduced seawater carbonate-saturation caused by short-lived injections of CO_2 from large igneous provinces that initiated OAEs. For OAE1a, this scenario also explains the retreat of carbonate platforms to low latitudes in the early Aptian, as sea-surface water typically has a higher carbonate saturation in warm, lower than in cooler, higher latitude waters. The gradual decrease of aragonite throughout the Cretaceous matches model simulations of seawater carbonate-saturation. An increase in the relative number of azooxanthellate coral genera following OAE1a and OAE2 suggests a disruption of photosymbiosis in the course of these global events due to high temperatures. However, the relative numbers of azooxanthellate genera continued to increase during the Late Cretaceous, when global temperatures declined. Due to the short residence time of major nutrients in seawater, these may have affected carbonate-producing ecosystems regionally. The recent patterns of benthic carbonate production being highest in oligotrophic environments cannot confidently be extrapolated to the Cretaceous.

Our database records ranges of genera at the substage level. Higher-resolution stratigraphical studies of neritic carbonate sequences are required to understand what aspect of environmental change in the sequence of events that unfolded in the context of OAEs caused the demise of benthic carbonate producers.

* Corresponding author.
E-mail addresses: thomas.steuber@ku.ac.ae (T. Steuber), loeser@paleotax.de (H. Löser), maparent@unina.it (M. Parente).

https://doi.org/10.1016/j.earscirev.2023.104341
Received 9 November 2022; Received in revised form 30 January 2023; Accepted 1 February 2023
Available online 10 February 2023

1. Introduction

The Cretaceous period (145–66 Ma) was an exceptional episode of Earth history, with high average sea-surface temperatures (Friedrich et al., 2012; Huber et al., 2018; Scotese et al., 2021), short periods of extreme warmth (Foster et al., 2018), and the highest sea level of the Phanerozoic (Miller et al., 2005). This coincided with widespread carbonate deposition both in pelagic and neritic environments.

The Cretaceous was the first period in Earth history when pelagic carbonates show a near to global distribution, documented by the widespread occurrence of limestones and chalks. In fact, the name 'Cretaceous' is derived from the Latin word 'creta', for chalk. The deposition of these carbonates is closely linked to the evolution of calcareous nannofossils, calcareous dinoflagellates and planktonic foraminifers. Calcareous nannofossils, which originated in the Late Triassic, became the most important carbonate producers in the marine pelagic realm where they constitute the most efficient carbonate rock-forming organisms of Earth history (e.g., Falkowski et al., 2004; Bown et al., 2004; Hay, 2004). Pelagic carbonate sedimentation also introduced a new, effective buffering mechanism for the global biogeochemical cycling of calcium carbonate through the dynamics of the lysocline (Zeebe and Westbroek, 2003; Ridgwell, 2005).

While the biotic composition of reefal communities and their major carbonate producers have remained remarkably similar since the mid Palaeozoic, variations in the relative importance of certain groups occurred (Stanley and Hardie, 1998). The Cretaceous was characterized by the rise of rudist bivalves as major benthic carbonate producers (Steuber, 2000), which dominated - or co-existed with - coral-algal-microbial communities in tropical shallow-water environments (Scott et al., 1990; Gili and Götz, 2018). The Cretaceous record of these benthic communities is punctuated by several episodes of demise and extinction (Skelton, 2003; Skelton and Gili, 2012), which appear to have coincided with recurrent episodes of oceanic anoxic events (OAEs). These were related to the activity of large igneous provinces, short-term pulses of increased atmospheric CO_2 concentrations, hyperthermals, and changes in the carbonate saturation of seawater (e.g., Schlanger and Jenkyns, 1976; Erba, 1994; Weissert et al., 1998; Zeebe, 2001; Jarvis et al., 2002; Leckie et al., 2002; Weissert and Erba, 2004; Erba et al., 2010; Jenkyns, 2010; Föllmi, 2012; Mutterlose and Bottini, 2013; Bauer et al., 2017; Foster et al., 2018; Matsumoto et al., 2022; Steuber et al., 2022). Most of the geochemical proxies that have helped to decipher the sequence of events during Cretaceous OAEs have, however, been derived from the more continuous pelagic and hemipelagic sedimentary sequences (e.g., Erba et al., 2010; Jenkyns, 2018; Sullivan et al., 2020; Castro et al., 2021). In contrast, and due to the rather discontinuous record of carbonate platforms, information about the precise timing and circumstances of the demise and recovery of Cretaceous carbonate platforms is still rather limited (e.g., Philip and Airaud-Crumiere, 1991; Parente et al., 2008; Föllmi, 2012; Skelton and Gili, 2012; Amodio and Weissert, 2017).

Global cooling or warming, ocean anoxia and acidification, and habitat loss related to sea-level change have been identified as the most important drivers of extinction in the geological record (Harnik et al., 2012). Some of these factors such as acidification can be triggered by bolide impacts or episodes of intense volcanism, the latter resulting in other perturbations of the carbon cycle causing global warming and ocean anoxia. Several of such potential triggers of extinctions occurred during the geologically short episodes of severe palaeoenvironmental perturbations that punctuated the Cretaceous, although only the end-Cretaceous mass extinction qualifies as one of the five great Phanerozoic extinction events. It significantly impacted almost all carbonate-producing biota discussed here and caused the final demise of the rudist bivalves. The end-Cretaceous extinction is not included in the present study, which instead focuses on the groups of biota that are characteristic for the unique types of Cretaceous carbonate sedimentation, and the response of these biota to internal perturbation of Earth's systems.

To test the response of major planktonic and benthic carbonate producers to Cretaceous environmental change, we have compiled stratigraphic ranges of genera of calcareous nannofossils (Fig. 1) and calcispheres, planktonic foraminifers (Fig. 2), species of dasycladalean algae (Fig. 3), genera of larger benthic foraminifers (LBFs, Fig. 4), corals (Fig. 5), and rudist bivalves (Fig. 6). The taxa investigated include photoautotrophic primary producers (calcareous nannofossils, calcispheres, dasycladalean algae), heterotrophic epifaunal suspension feeders (rudist bivalves), as well as epifaunal detritus and suspension feeders, and predators (LBFs, corals). Some groups were photosymbiotic, such as many corals and LBFs, and possibly a few rudist bivalves, with photosymbiosis being typically linked to high calcification rates. Large differences among the groups studied also exist in the mode of calcification. Therefore, different responses to changing environmental conditions that affect the precipitation of aragonite, low-Mg and high-Mg calcite must be expected. Here, the observed patterns of diversity will be compared with records of Cretaceous environmental change, aiming at the identification of potential drivers of the rise and demise of Cretaceous carbonate producers and their characteristic depositional systems. This addresses fundamental questions of biogeodynamics, e.g., to what extent geological process have affected the evolution of life and vice versa (Spencer, 2022). Our data may also provide information to evaluate future extinction risks of modern carbonate-producing biota, specifically related to anthropogenic climate change and compositional changes of seawater (Finnegan et al., 2015).

2. Methods

The datasets consist of ranges of genera for calcareous nannofossils, calcispheres, planktonic foraminifers, LBFs, corals, rudist bivalves, and species of dasycladalean algae. Methods used for the compilation of stratigraphical ranges, defined by the first and last occurrences of genera, are described separately for each group. All ranges and data adopted from other sources are calibrated to the GTS 2012 time scale (Gradstein et al., 2012). If applicable, ranges for taxa with skeletons, shells, or tests of different original carbonate minerals (low-Mg calcite, high-Mg calcite, aragonite) are distinguished, such as for LBFs and rudist bivalves.

In contrast to other approaches to evaluate diversity patterns in the fossil record that utilize large databases with heterogenous quality, we did not apply methods such as random subsampling (e.g., Alroy et al., 2001). Our data acquisition is based on an expert evaluation of available occurrence data to construct taxon ranges that reflect the current state of knowledge. As the range distribution of genera is quite different for the taxonomic groups studied, we assume that the observed trends are robust, and not the result of any preservation or sampling artifacts. These have been shown to significantly affect raw diversity data (Raup, 1975), particularly on long, Phanerozoic time scales. The significantly different sample sizes when comparing nannofossils (e.g., coccoliths), microfossils (e.g., LBFs and dasycladalean algae), and macrofossils (corals and rudists), renders uniform statistical approaches difficult (Yasuhara et al., 2017) and may result in inappropriate manipulations of true patterns.

2.1. Calcareous nannofossils, calcispheres

The term calcareous nannofossil includes two different taxonomic groups, coccoliths and nannoliths. Coccoliths, which are produced by haptophyte algae, consist of two different morphological groups, the holococcoliths and the heterococcoliths. The latter are more common in the fossil record. Nannoliths are calcareous skeletons of unknown taxonomic affiliation with a diversity much lower than that of coccoliths. Classification and stratigraphic ranges of calcareous nannofossils used here follow Perch-Nielsen (1985), the Nannotax3 database of Young et al. (2021) and the Farinacci catalogue (Farinacci and Howe, 1969–2022). Calcispheres are calcitic cysts, attributed to

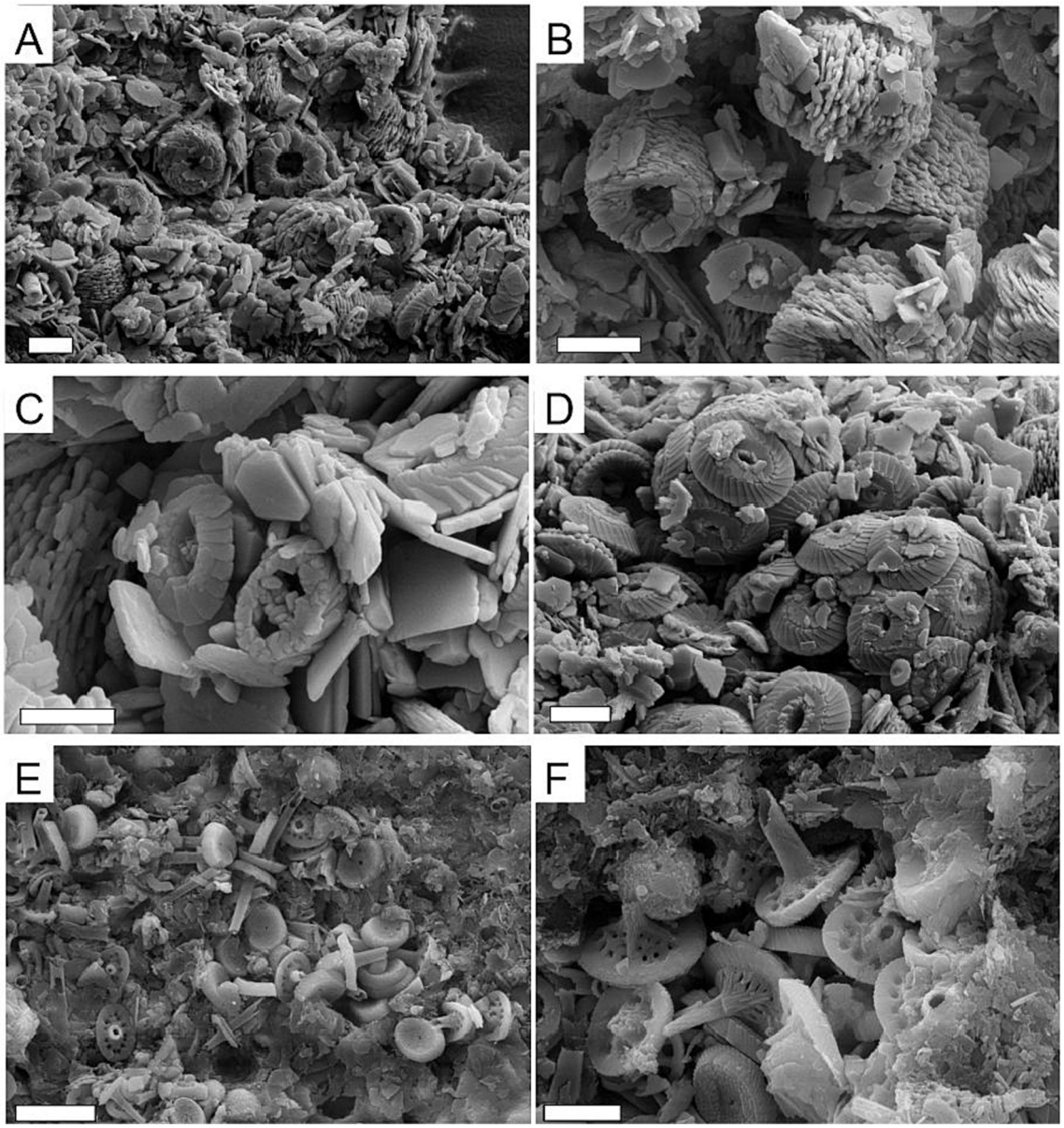

Fig. 1. Cretaceous calcareous nannofossils. A. In the centre plan views of four nannoliths (*Nannoconus*) and rarer heterococcoliths (upper left, lower right), Barremian of the North Sea; scale bar is 4 μm. B. Side views of four nannoliths (*Nannoconus*) and rare heterococcoliths, Barremian of the North Sea; scale bar is 4 μm. C. Two heterococcoliths in the centre (*Biscutum constans* left, *Zeugrhabdotus diplogrammus* right), fragments of heterococcoliths, Barremian of the North Sea; scale bar is 2 μm. D. Two coccospheres (centre) and isolated coccoliths of heterococcoliths (*Watznaueria barnesiae*), Barremian of the North Sea; scale bar is 4 μm. E, F. Heterococcoliths (*Rhagodiscus asper*, *Cretarhabdus conicus*), Barremian northern Germany; scale bar is 10 μm (E) and 4 μm (F).

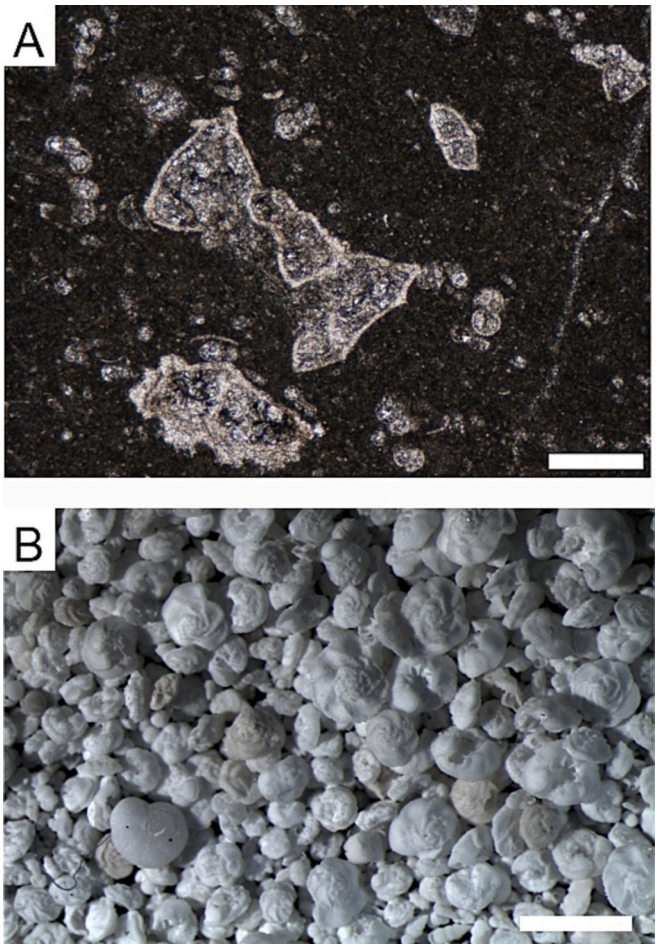

Fig. 2. Cretaceous planktonic foraminifers. A. thin section microphotograph of *Dicarinella asymetrica*; Santonian, *Dicarinella asymetrica* Zone, Scaglia Bianca Formation, Bottaccione section, Italy. Scale bar is 200 µ. B. Globotruncanid assemblage, including rare benthic foraminifers, washing residue; Campanian, *Globotruncana neotricarinata* Zone, Shatsky Rise, Pacific Ocean. Scale bar is 1 mm.

dinoflagellates. The evaluation of calcispheres is based on the taxonomic concept of Elbrächter et al. (2008) and an electronic index of fossil dinoflagellate cysts – Dinoflaj3. The group 'incertae sedis' includes calcareous tests of 80–200 µm size, which have been assigned to the informal group 'Gilianelles' (Odin, 2011). Earlier, these microproblematica have been interpreted as dinoflagellate cysts.

2.2. Planktonic foraminifers

Ranges of genera of planktonic foraminifers are from Bown et al. (2022) and reported here at the stage level. The trends resulting from these data are similar to a more detailed compilation of numbers of morphospecies binned to 1 myr intervals (Lowery et al., 2020).

2.3. Dasycladalean algae

The ranges of Cretaceous species of dasycladalean algae (order Dasycladales Pascher, 1931) have been compiled starting from Granier and Deloffre (1993) and updated based on a critical review of papers published between 1993 and July 2021. Species instead of genera were evaluated for this group, because many genera are monospecific, and most others include very few species.

2.4. Larger benthic foraminifers

Ranges of Cretaceous LBFs have been compiled based on the monographs of Loeblich and Tappan (1988) and BouDagher-Fadel (2018) and refined by incorporating data on the genus-level taxonomy and on chronostratigraphic ranges based on a critical review of papers published between 1988 and July 2021.

2.5. Corals

The ranges of genera are from the compilation of Löser (2016), and based on material that was examined by HL. Material without an exact stratigraphic control was not included. Uncertain taxa, for example those lacking type material, or published illustrations and description that did not allow unequivocal assignation to a genus, were excluded. The ranges have been modified from Löser (2016) when new material was available.

2.6. Rudist bivalves

Ranges of rudist genera (Hippuritida Newell, 1965) are adopted from Steuber et al. (2016). This compilation is based on biostratigraphy, graphic correlation, and strontium isotope stratigraphy, as described in detail in Steuber et al. (2016).

3. Results

3.1. Calcareous nannofossils, calcispheres

The number of coccolith genera (heterococcoliths, holococcoliths) shows a gradual increase throughout the Early Cretaceous, with a first peak in the Albian (Fig. 7). This is followed by a minor decline in the Cenomanian–Santonian. The number of genera reaches its Cretaceous maximum in the Campanian, followed by a minor decline up to the late Maastrichtian. The distribution of nannoliths closely resembles that of the coccoliths. Their genera steadily increase in number in the Early Cretaceous and reach a first peak in the Albian, followed by a minor decrease in the Cenomanian. Numbers increase again in the Turonian and are relatively stable up into the Campanian, followed by a minor reduction in the Maastrichtian. The diversity pattern of calcareous dinoflagellates (calcispheres) shows a very similar pattern. Following a gradual increase throughout the Early Cretaceous, they reach a first maximum in the late Albian. High values characterize the Cenomanian–early Campanian interval, followed by a mid-Campanian–early Maastrichtian decline. Numbers increase again in the late Maastrichtian. Incertae sedis, comprising the Gilianelloids occur in the late Campanian and early Maastrichtian. There are no significant changes in the number of calcareous nannofossil genera at the stratigraphic levels of OAEs.

3.2. Planktonic foraminifers

The number of genera of planktonic foraminifers increases throughout the Early Cretaceous and until the Coniacian (Fig. 7). Following a minor decrease in the Santonian, numbers increase again to reach the Cretaceous peak in the Campanian. This is followed by a minor decrease in the Maastrichtian. The extinction event at the Cretaceous Palaeogene boundary was sudden and catastrophic (Molina, 2015), and the relatively high number of Danian taxa reflects recovery of diversity during the earliest Palaeogene stage.

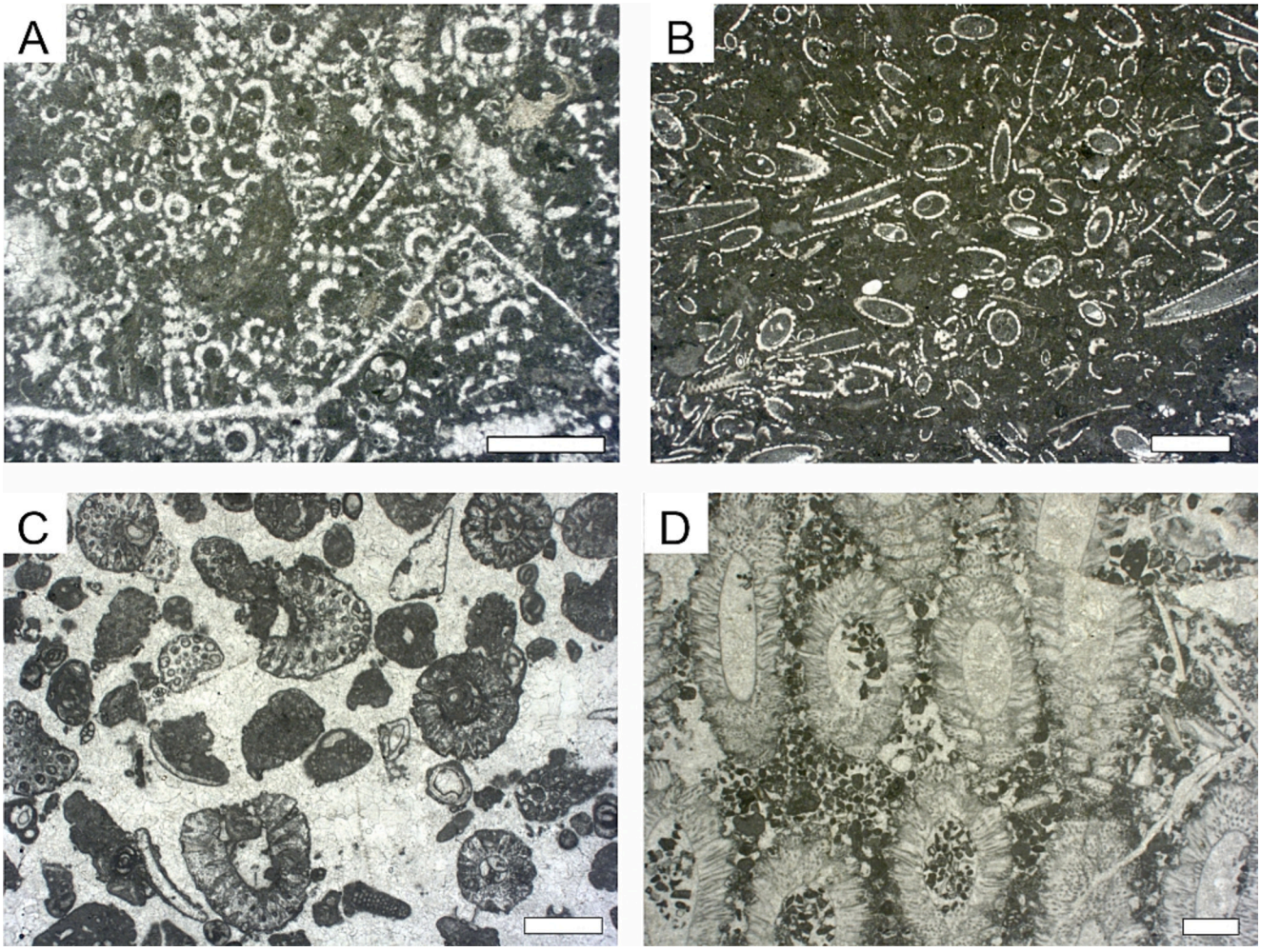

Fig. 3. Thin-section microphotographs of Cretaceous dasycladalean algae; optical microscope, parallel nicols. A. Very rich assemblage dominated by *Salpingoporella annulata*; Hauterivian, Monte Motola, southern Apennines, Italy. B. Monospecific assemblage of *Salpingoporella dinarica*, one of the few dasycladalean algae producing a skeleton of low-Mg calcite; lower Aptian, southern Apennines, Italy. C. *Morelletpora turgida*; Albian, Monte Lo Cugno, southern Apennines, Italy. D. Very rich monospecific assemblage of *Linoporella capriotica*; Hauterivian, Capri Island, Italy. Scale bar is 1 mm for all microphotographs.

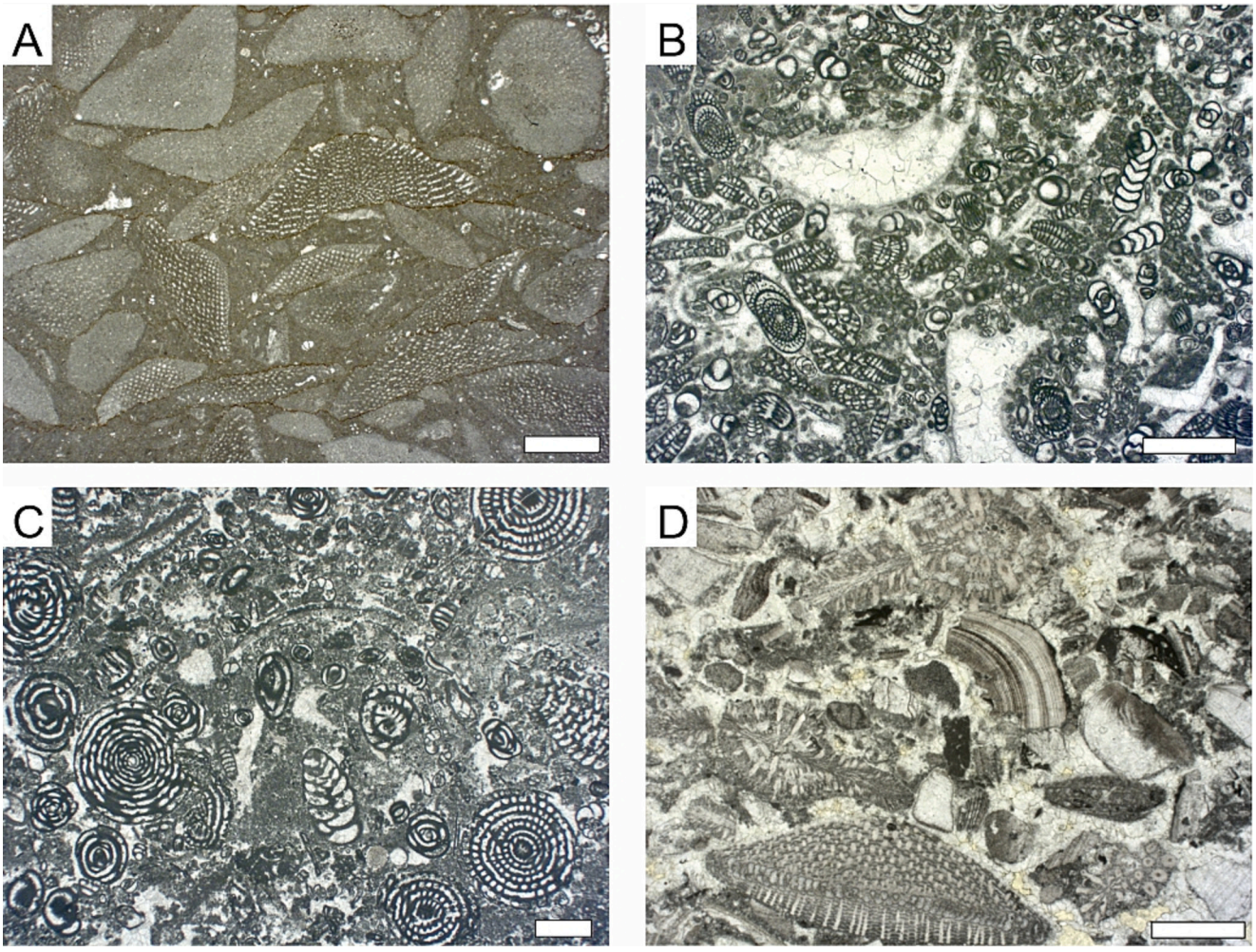

Fig. 4. Thin-section microphotographs of Cretaceous larger benthic foraminifers; optical microscope, parallel nicols. A. Dense accumulation of low-conical orbitolinids; upper Aptian, "*Orbitolina* level", Monte Coccovello, southern Apennines, Italy. B. Very rich and diverse assemblage with *Cuneolina*, *Sellialveolina* and *Pseudorhapydionina*; middle Cenomanian, Monte Lo Cugno, southern Apennines, Italy. C. Very rich and diverse assemblage with *Cisalveolina fraasi* and *Chrysalidina gradata*; upper Cenomanian, Monte Cerreto, southern Apennines, Italy. D. Platform margin microfacies with calcareous perforate larger benthic foraminifers (*Orbitoides* and *Siderolites*) and fragments of rudists shells. Maastrichtian, Ciolo Cove, Salento peninsula, Italy. Scale bar is 1 mm for all microphotographs.

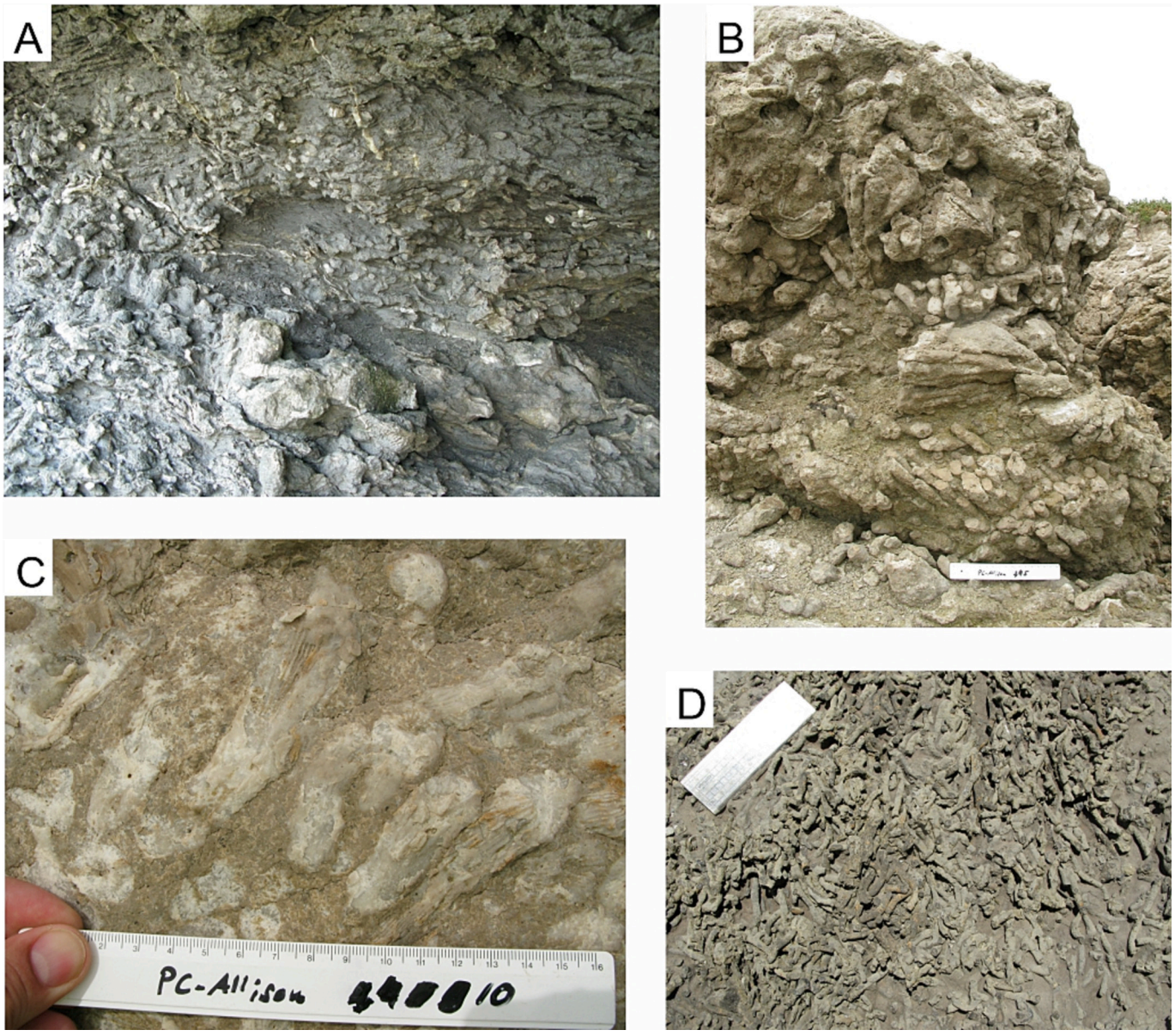

Fig. 5. Outcrop photographs of Cretaceous corals. A. Massive coral colonies of the genus *Thalamocaeniopsis* within coral thickets of the genus *Actinastraeopsis* in live position; Lower Albian, Cantandria, Cabo de Ajo, Spain. B. Dendroid growing, cerioid corals (*Thalamocaeniopsis*); Lower Albian, Alisitos Formation, Baja California, Punta China, Mexico. C. Phaceloid corals (*Apoplacophyllia*); Lower Albian, Alisitos Formation, Baja California, Punta China, Mexico. D. Coral thickets, *Actinastraeopsis* sp.; Aptian/Albian boundary interval, País Vasco, Vizcaya, Gamecho, Playa de Laga, Spain.

3.3. Dasycladalean algae

The number of dasycladalean species increases during the Early Cretaceous to form a broad peak during the Barremian–early Aptian, and subsequently declines to a minimum in the Campanian, followed by a minor increase in the Maastrichtian (Fig. 8).

3.4. Larger benthic foraminifers (LBFs)

The overall number of genera of LBFs (Fig. 8) increases throughout the Early Cretaceous until a first peak in the early Aptian, with a minor reduction in the Hauterivian. Numbers remain relatively low throughout the late Aptian–Albian and increase again in the Cenomanian. A sharp reduction occurs at the Cenomanian/Turonian boundary, followed by an increase to the Cretaceous peak in genera numbers in the late Campanian. Microgranular agglutinating taxa are dominant until the end of the Cenomanian. Aragonitic hyaline genera occur in relatively small numbers in the Early Cretaceous and disappear at the end of the Cenomanian. Low-Mg calcite hyaline taxa are represented by a few genera in the Berriasian–early Aptian, appear again in the Cenomanian, and reached highest numbers in the late Campanian. High-Mg calcite porcelaneous genera increase from the Aptian–Cenomanian, followed by a sharp reduction at the Cenomanian/Turonian boundary and an increase to a maximum in the late Campanian.

Regarding their original test mineralogy, porcelaneous taxa are considered as consisting of high-Mg calcite, based on analysis of recent species (de Nooijer et al., 2009; Sadekov et al., 2014). Hyaline genera are either calcite (lamellar rotaliids and “mono-crystalline” spirillinids) or aragonite (trocholinids). Agglutinated Textulariida have a low-Mg calcite cement (Dubicka, 2019).

3.5. Corals

Corals maintain a high number of genera throughout the Cretaceous

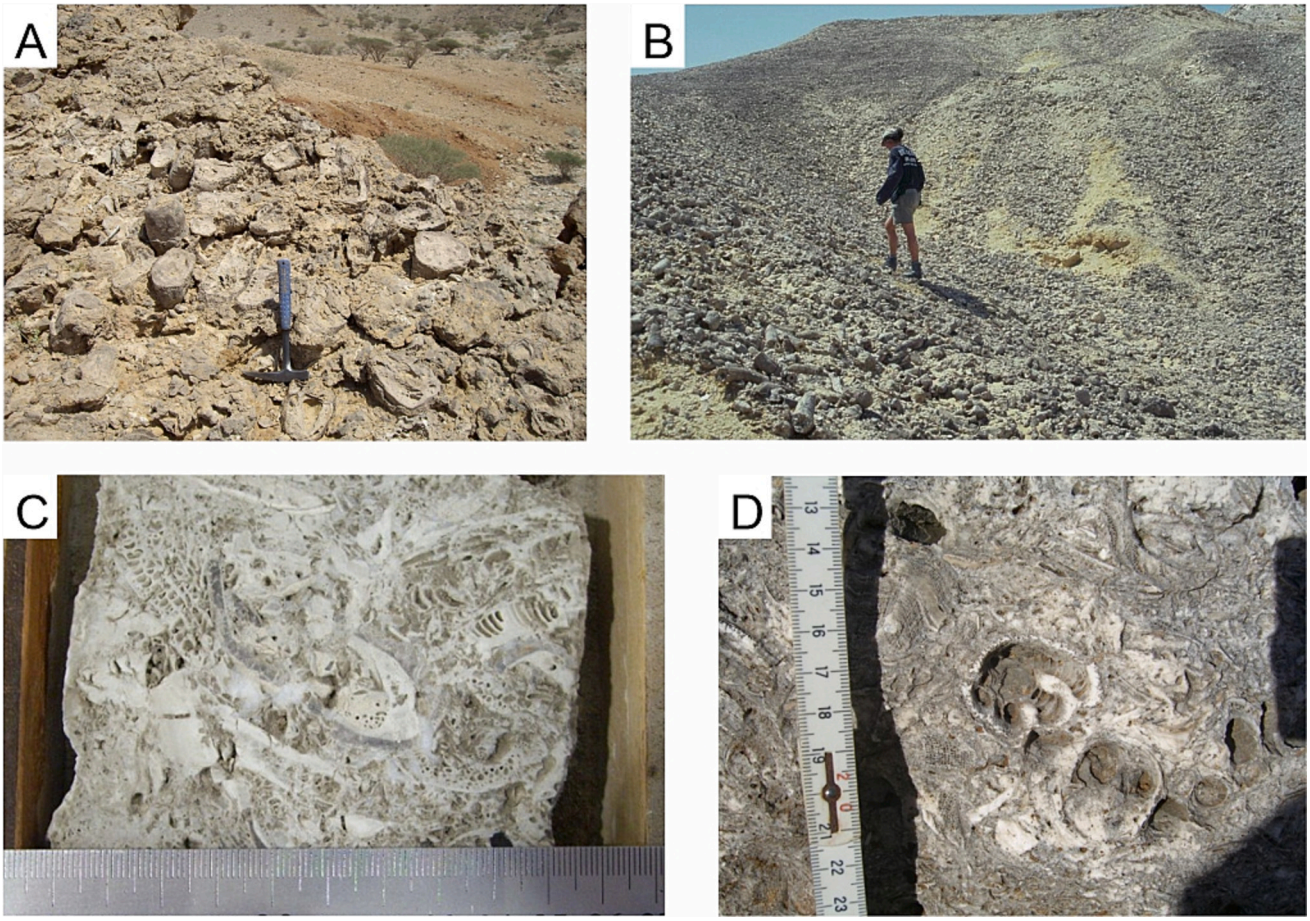

Fig. 6. Cretaceous rudist bivalves. A. Bedding plane view of rudists in vertical live position, predominantly *Dictyoptychus*, with some Radiolitidae; Maastrichtian, Jebel Sumeini, Oman. B. Hillslope covered with shells of *Vaccinites*, eroded from a c. 1 m thick lithosome exposed at the top of the hill; Saiwan, Oman. C. Reworked shells of caprinid rudists, predominantly *Offneria*; well core of Lower Aptian Shu'aiba Formation, UAE. D. Reworked rudist debris, predominantly Radiolitidae, hippuritid rudist in centre of photograph; Turonian, Kefalonia Island, Greece. See http://www.paleotax.de/rudists/ruform.htm for further images of rudist formations.

(Fig. 8), with an overall trend of increasing numbers until the Cenomanian, followed by a moderate decline until the late Maastrichtian (Fig. 8). Superimposed on this trend, moderate reductions occur in the Berriasian, at the early/late Aptian boundary, in the early Turonian, and early Campanian. Two of these reductions are stratigraphically related to OAE1a and OAE2. Azooxanthellate corals occur with only a few genera until the early Aptian, increase substantially in the late Aptian and again to a Cretaceous peak in the Maastrichtian.

3.6. Rudist bivalves

The number of rudist bivalve genera increases almost exponentially until a peak in the late Campanian, and then moderately decreases until the late Maastrichtian, followed by extinction at the K/P boundary (Fig. 8). This overall pattern is punctuated by significant reductions in the number of genera stratigraphically related to the Weissert event, OAE1a, and OAE2. Genera with calcite-dominated shells appeared first in the Hauterivian, and increase in numbers until a peak in the late Campanian. Calcite-dominated genera were not affected by the reduction in genera numbers in the Valanginian, at the early/late Aptian, and the Cenomanian/Turonian boundary. Therefore, reductions in total numbers of genera are exclusively caused by the demise of aragonite-dominated genera, and taxa with no specific mineral dominance at the Cenomanian-Turonian transition. Aragonite-dominated genera decrease to <10% after the Weissert event and OAE2, and to 13% after OAE1a.

3.7. General patterns

Comparing the general patterns in the evolution of the number of genera, despite their different habitats, autecology, and shell mineralogy, similar trends are obvious for calcareous nannofossils, calcispheres, planktonic foraminifers, and corals. Reductions in the number of genera are minor when compared to the other groups of organisms studied here, and the overall trend broadly follows the evolution of sea level (Fig. 7). All other groups (rudist bivalves, LBFs, dasycladalean algae) show more accentuated changes in diversity, with periods of reductions in the number of taxa related to periods of global demise of carbonate platforms and oceanic anoxic events (Fig. 9). Those groups that employed either calcite or aragonite (LBFs) or both minerals (rudist bivalves) in calcification show a general reduction in the abundance of aragonite during the Cretaceous. A significant decline of purely aragonitic or aragonite-dominant taxa is evident for the OAE intervals. Low-Mg calcitic perforate and hyaline LBFs show no significant reduction, and calcite dominated rudists increase in the number of genera during these time intervals. The bi-mineralic rudists show the most pronounced pattern of changing aragonite dominance.

The very different patterns of genus-level diversity of corals and rudists may appear unexpected. Both are frequently considered to be 'reef-building biota', with rudists replacing corals in this role during the Cretaceous. This view has been shown to be erroneous (Gili et al., 1995; Skelton et al., 1997; Gili and Götz, 2018), as rudist were gregarious sediment dwellers, unable to construct frameworks that were

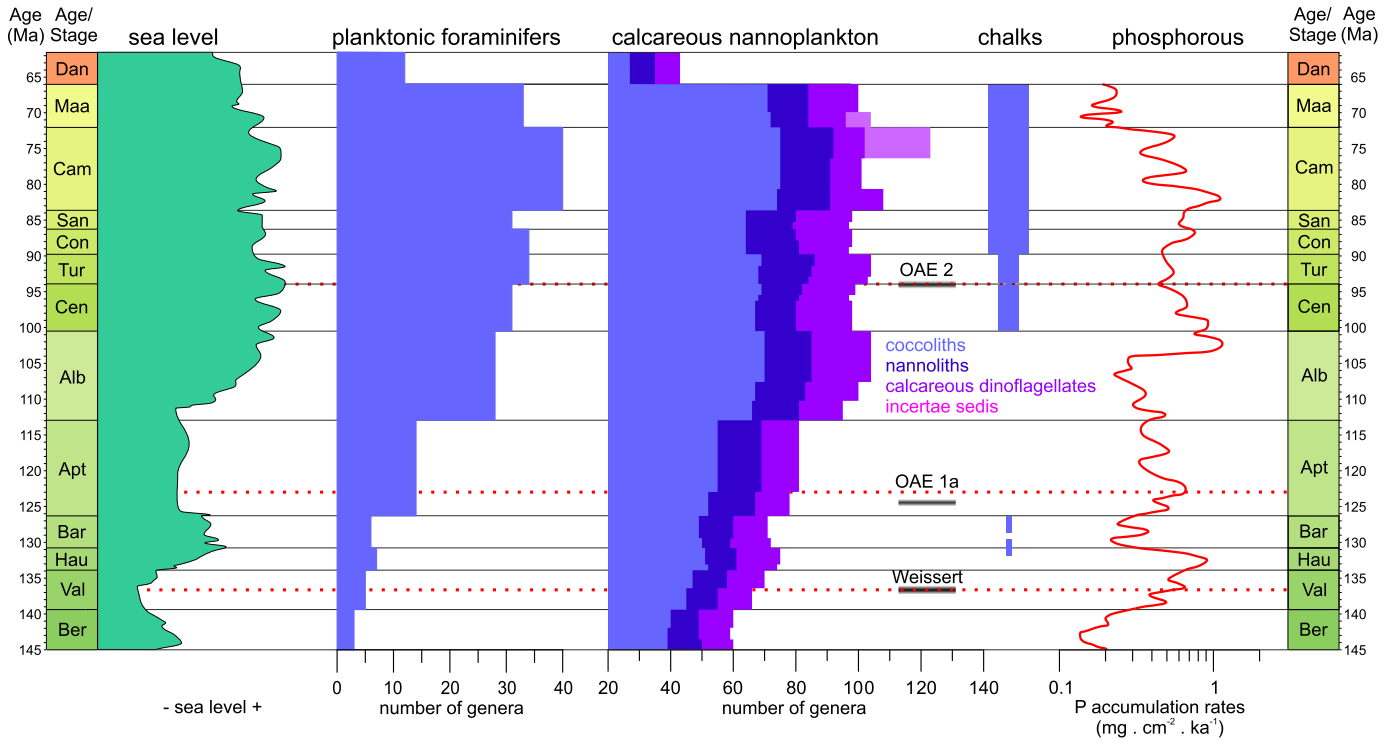

Fig. 7. Cretaceous–Danian sea-level change (Gradstein et al., 2012), ranges of genera of Cretaceous–Danian planktonic foraminifers, calcareous nannofossils, Cretaceous distribution of northern-hemisphere chalks, and phosphorous accumulation rates in marine sediments (Föllmi, 1995). Red dashed horizontal lines indicate extinction events. See text for sources of data. (For interpretation of the references to colour in this figure legend, the reader is referred to the web version of this article.)

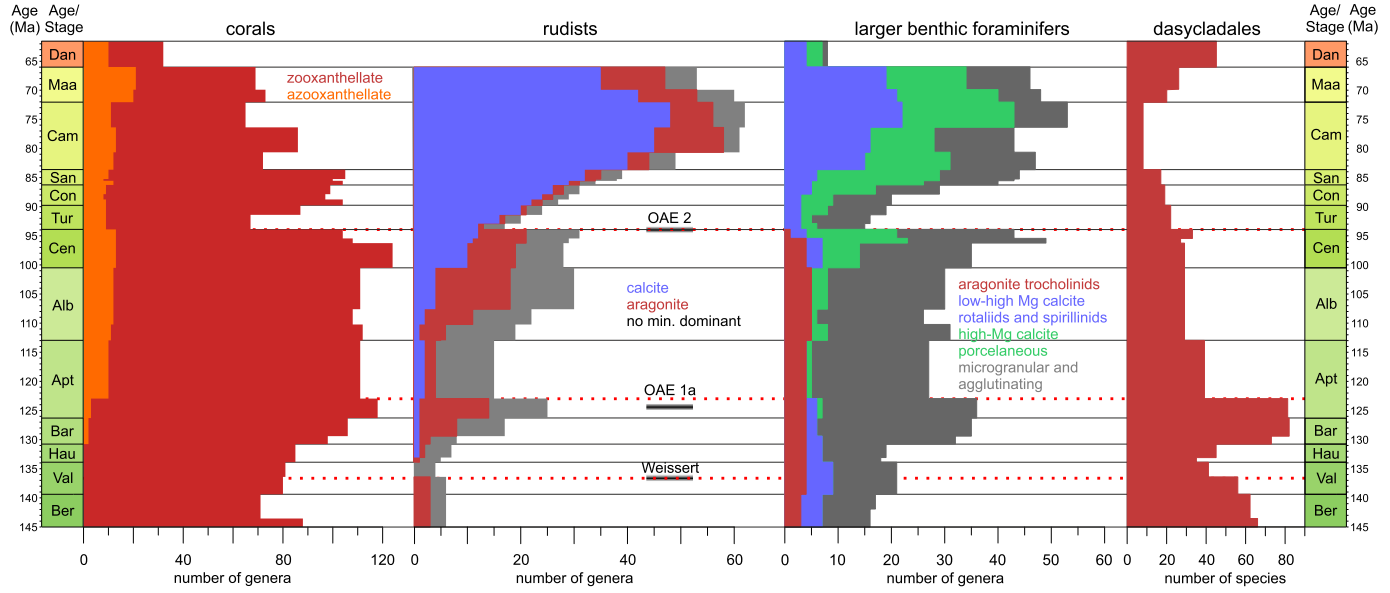

Fig. 8. Ranges of genera of Cretaceous–Danian corals, rudist bivalves, larger benthic foraminifers (LBFs), and species of dasycladalean algae. The dominant carbonate mineral of genera of rudist bivalves and LBFs are shown in different colours. Red dashed horizontal lines indicate extinction events. See text for sources of data. (For interpretation of the references to colour in this figure legend, the reader is referred to the web version of this article.)

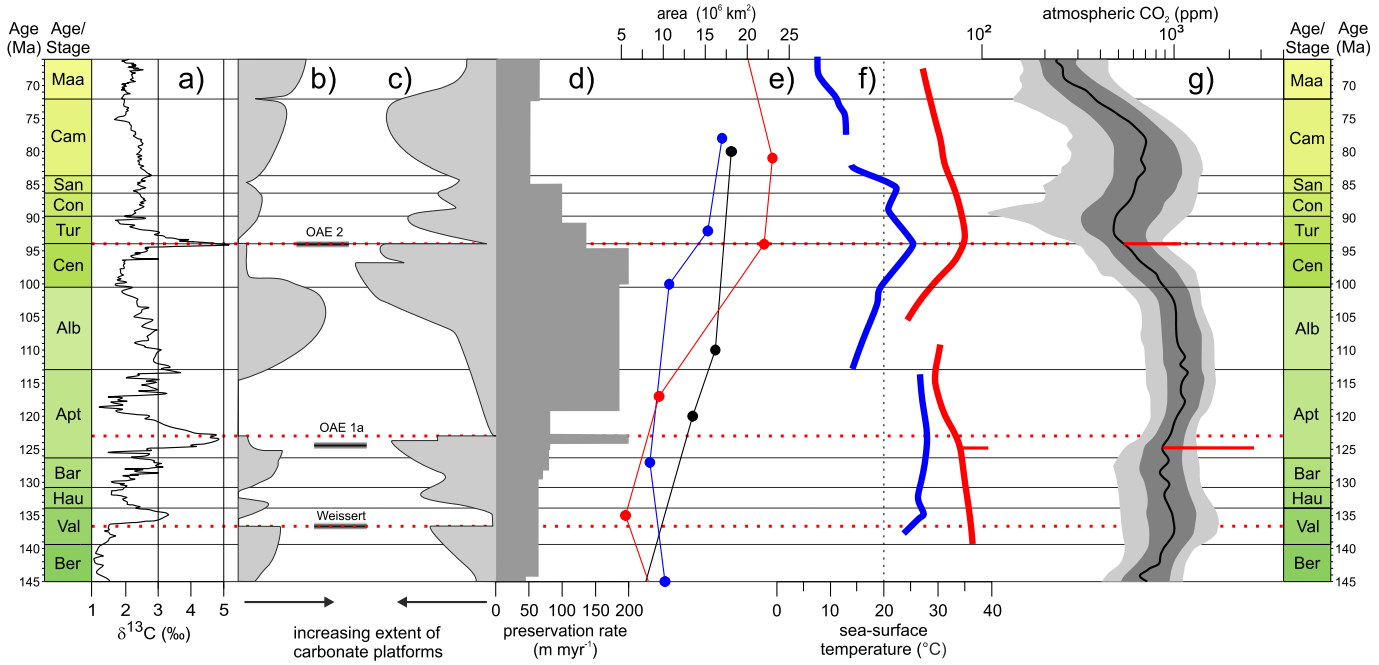

Fig. 9. Cretaceous carbon-isotope record (a, from Steuber et al., 2016); extent of carbonate platforms in the Americas (b, 'new world'), and Europe, north Africa and the Middle East (c, old world, from Skelton, 2003, not quantified); neritic carbonate-preservation rates (d, Pohl et al., 2020); (e) surface area of carbonate platforms as simulated by Pohl et al. (2019, black line), trends published by Kiessling et al. (2003; blue line); flooded continental areas from Cao et al. (2017, red line); (f) evolution of sea-surface temperatures (mean values) estimated from $\delta^{18}O$ values of planktonic foraminifers and Tex_{86}, from O'Brien et al. (2017) for low palaeolatitudes (< 30°, red lines) and high palaeolatitudes (> 48°, blue lines), red horizontal bar at the level of OAE 1a indicates short-term deviation from mean value; (g) atmospheric CO_2 concentrations (Foster et al., 2017), red horizontal lines indicate LIP-related short-term increase of atmospheric CO_2 concentrations of 1000–2000 ppm during OAE1a and 370–500 ppm during OAE2 (Foster et al., 2018). Red dashed horizontal lines indicate extinction events. (For interpretation of the references to colour in this figure legend, the reader is referred to the web version of this article.)

substantially elevated above the sediment surface. Nevertheless, corals and rudists frequently co-occur, although Early Cretaceous corals may have preferred slightly deeper environments than rudists (Scott et al., 1990). Neither group is restricted to carbonate-platform environments and corals and rudists also occur or co-occur in mixed siliciclastic-calcareous depositional systems. Therefore, other factors must be considered to have controlled the different pattern of ranges of corals and rudists.

For several of the groups studied here, patterns of taxonomic and ecologic turnover have been recognized previously on a high-resolution scale, below the substage level. In a high-resolution, species-level analysis of calcareous plankton diversity, Lowery et al. (2020) noted that extinction and turnover was decoupled from that of the benthos. Species turnover in planktonic foraminifers around OAE1a and OAE2 were related to changes in surface biological productivity, vertical stratification, carbonate chemistry, and nutrients caused by eustatic sea-level change (Kuroyanagi et al., 2020). Declines and shifts in the species composition have been observed for calcareous nannofossils throughout the Valanginian Weissert Event (Mattioli et al., 2014), at the onset of the Aptian OAE1a (Erba, 2004; Erba et al., 2010) and across the Cenomanian OAE2 (Leckie et al., 2002; Linnert et al., 2010). The declines seem to be mainly driven by an increase of the nutrient supply. A significant decline of the nannolith *Nannoconus*, a genus which became extinct in the Albian, has been observed for the Weissert Event, OAE1a, and OAE1b (latest Aptian; Leckie et al., 2002; Huber and Leckie, 2011), suggesting bio-calcification crises. In addition to CO_2 and nutrient availability, bio-limiting metals may have played a role. Alternatively, reduced preservation of calcareous nannofossils during OAEs may have affected abundance patterns (Slater et al., 2022).

For LBFs a turnover has been described for the onset of OAE2 (Parente et al., 2008), and for rudist bivalves during OAE1a (Strohmenger et al., 2010; Skelton and Gili, 2012) and OAE2 (Philip and Airaud-Crumiere, 1991). These studies provide important clues for the cause-effect relationships of these turnovers, and will thus be referred to in the following discussion. Our data do not cover these specific intervals in detail, they rather record the long-term evolution of Cretaceous carbonate production on a lower stratigraphic resolution on the substage-level.

4. Discussion

4.1. Preservation and collection bias

In comparison to calcite, aragonite is more susceptible to diagenesis and is either replaced by diagenetic calcite or dissolved, potentially introducing a taphonomic bias (e.g., Wright et al., 2003). This bias is obvious particularly on long Phanerozoic time scales, and such data have been detrended to account for preferential preservation of originally calcitic fossils (e.g., Kiessling et al., 2008). Considering the comparatively short duration of our records, and no evidence for a trend of decreasing numbers of originally aragonitic taxa with time, we assume that a preservation bias has not significantly affected our dataset (cf. Foote et al., 2015; Eichenseer et al., 2019). It may have affected corals, but the bi-mineralic rudist are typically preserved even if the inner aragonitic shell layers are dissolved or calcitized. Aragonitic foraminifers presumably have a more incomplete preservation record than calcitic taxa (Rigaud et al., 2021), but this potential bias cannot be quantified reliably. Among the groups studied, the record of dasycladalean algae was possibly most affected by a taphonomic bias, although the number of species increases with increasing age. As facultative calcifiers (Berger and Kaever, 1992), environmental factors and taphonomic effects will have contributed to their fossil record. The

preservation mode of the c. 3–6 μm sized calcareous nannofossils, composed of low Mg-Calcite, is a standard issue addressed in many nannofossil publications. Preservation may bias the taxonomic composition of nannofossil assemblages even in consecutive samples of stratigraphic sections due to carbonate dissolution or lithological changes. Heterococcoliths are often better preserved than holococcoliths, due to the different crystallographic architecture of these two coccolith types. The near-to-global record for at least the Late Cretaceous sequences by ODP/DSDP/IODP gives access to a robust dataset from time equivalent locations around the world, excluding a diagenetic bias of the record discussed here.

The broad pattern of generic diversity of calcareous nannofossils, calcispheres, planktonic foraminifers, and corals traces the evolution of sea level during the Cretaceous (Figs. 7, 8). This may reflect a sampling bias as more marine rocks are preserved for sampling from episodes of high sea level (e.g., Smith et al., 2001). Alternatively, flooded continental margins and marine gateways that developed during the Late Cretaceous across north Africa, Eurasia, and north America resulted in new dispersal routes and, combined with high sea-surface temperatures, in the expansion of favourable environments.

There is considerable evidence that the observed variation in marine diversity, particularly on long Phanerozoic time-scales, may be an artifact of variation in the amounts of rock available for sampling (Peters and Foote, 2001). Correcting occurrences for available rock volumes would require complex estimates of largely unknown data. For example, the available rock volume of 'chalk', typically the result of accumulations of rock-forming quantities of coccoliths, would have no relation to the occurrence of rudist bivalves. Considering the debate about artifacts in the fossil record related to sampling and preservation biases (e.g., Raup, 1976; Jackson and Johnson, 2001; Peters et al., 2013), patterns of proportional diversity as seen in our dataset, should not be affected (Bambach et al., 2002).

4.2. Calcification and autecology

To evaluate the disparate patterns in the observed diversity dynamics, it is important to consider to what extent physiological processes control the precipitation of skeletal carbonate formation in the groups discussed here. This ranges from a minimum control in dasycladalean algae, where calcification is extracellular and driven by localized alkalinization by removal of CO_2 during photosynthesis (Borowitzka, 1986), to precipitation from an extrapallial fluid in bivalves. In the latter, biological control facilitates chemical modification of the extrapallial fluid, which is isolated from ambient seawater, and controls the formation of various structures of bi-mineralic shells (aragonite and low-Mg calcite). Calcification may be of different autecological significance, ranging from facultative calcification in dasycladalean algae (Berger and Kaever, 1992) to the complex bi-mineralic shell structures of rudist bivalves that functioned to channel inhalant and exhalant water current, provided protection against bioeroders, and were adapted to clinging, recumbent, or elevator life habits (Gili and Götz, 2018). The groups investigated include autotrophs such as the calcareous nannofossils and dasycladaleans, while all others are heterotrophs among which some will have been mixotrophic, relying to varying degrees on photosymbiosis for metabolism and calcification.

Previously, Bambach et al. (2002) introduced the concept of taxa that are 'buffered' or 'unbuffered' against physiological changes. Various aspects of physiological stress must be considered that will not uniformly affect different taxa, such as the impact of high temperatures on coral and LBF photosymbiosis and calcification, even at favourable seawater aragonite saturation (Kawahata et al., 2019). There may also be enhanced vulnerability when calcification is required at larval stages (e.g., in bivalves; Byrne and Przeslawski, 2013). As background for further discussion, we have summarized the main aspects of the autecology and mode of calcification of Cretaceous carbonate producers. Improved understanding of these aspects, particularly in taxa now extinct, will enhance future interpretations of the observed diversity patterns.

4.2.1. Calcareous nannofossils, calcispheres

Calcifying haptophytes (coccolithophores) most likely originated in the Triassic, with a diploid phase (heterococcoliths) and a haploid phase (holococcoliths) producing morphologically different calcifying cells during their life cycle. The calcification of heterococcoliths is a highly complex biomineralization process, which clearly differs from that of holococcoliths with respect to crystal nucleation and growth (Young et al., 1999; Billard and Inouye, 2004). The calcification process reduces the amount of OH^- ions generated during photosynthesis. Heterococcoliths, which consist of variably shaped crystal units, are formed inside the cell and are then extruded to form a complex exoskeleton, with physiological effects on coccolith physicochemical composition (Hermoso, 2015). Coccolith formation occurs in Golgi vesicles. Holococcoliths are composed of small, equidimensional calcite crystals, and calcification is extracellular (Young et al., 1999). Nannoliths are a taxonomically heterogenous group, having calcareous skeletons different from those of hetero- or holococcoliths. Some nannoliths are perhaps related to heterococcoliths, others to holococcoliths.

Calcispheres are the calcitic cysts of calcareous dinoflagellates. Biomineralization takes place either externally on the substrate of the cell surface or internally in vesicles (Elbrächter et al., 2008). Biomineralization in calcareous dinoflagellates is strongly controlled at the cellular level.

Global production of calcite in recent oceans by calcareous nannofossils is not well constrained but they make up the major fraction of carbonate in marine pelagic and hemipelagic sediments. Roughly half of the oceanic $CaCO_3$ exported from the sea surface is thought to be produced by calcareous nannofossils (Schiebel, 2002; Broecker and Clark, 2009).

4.2.2. Planktonic foraminifers

Planktonic foraminifers are omnivorous, heterotrophic protozoans. Photosymbiosis is common among many modern taxa, but probably developed only in the latest Cretaceous (D'Hondt and Zachos, 1998; Houston and Huber, 1998; Bornemann and Norris, 2007).

Modern planktonic foraminifera show a distinctive biogeographic provincialism with a bipolar distribution of specific species. The most diverse modern assemblages are found in the subtropical and temperate ocean (Schmidt et al., 2004). Exported carbonate production is linked to trophic levels; oligotrophic waters of the subtropical gyres are characterized by the lowest, and mesotrophic waters of temperate and subpolar waters by the highest production, although diversity is highest in the oligotrophic subtropical gyres (Schiebel and Hemleben, 2017). Ecological conditions in modern eutrophic waters are more complex because of the negative effects of high primary production on photosymbiotic species. Vertical distribution of planktonic foraminifers depends on the availability of food, and the requirement for light in photosymbiotic taxa. Deep-dwelling planktonic foraminifers live well below the pycnocline down to 400 m water depth, where they experience more stable environmental conditions than shallow-dwelling taxa (Schiebel and Hemleben, 2017). Mixed-layer to sub-thermocline depth habitats were identified in different genera of Campanian–Maastrichtian planktonic foraminfers by stable isotope analyses of test carbonate (Abramovich et al., 2003). Most modern species are eurythermal, with an optimum temperature of c. 10 °C (Lombard et al., 2011).

Tests of planktonic foraminifers are made of calcite and organic layers. Test size of planktonic foraminifers is positively correlated with mean annual water temperature. This general pattern is regionally modified by trophic levels and surface water stratification (Schmidt et al., 2004). Biomineralization is assumed extracellular, and calcite is deposited on a primary organic membrane, which is secreted within a cytoplasmic extension of the main cell mass that encloses seawater. Vaterite has been shown to be the unstable precursor of calcite

precipitation (Jacob et al., 2017). The bulk of the test mass, however, is produced by the addition of calcite layers to the outer test surface (e.g., during the formation of new chambers and during gametogenesis). Test mass is generally positively affected by high seawater alkalinity, *p*H and temperature (Schiebel and Hemleben, 2017).

Langer (2008) reports that benthic and planktonic foraminifers currently produce approximately 1.4 billion tonnes of calcium carbonate per year, which ends up buried in oceanic sediments, representing approximately 25% of the global-ocean carbonate production.

4.2.3. Dasycladalean algae

Recent dasycladalean algae are facultative calcifiers. In their natural habitat some species produce a thick calcareous skeleton, while others produce only a very thin coat, or may be uncalcified (Berger and Kaever, 1992). Calcification occurs mainly by extracellular precipitation of aragonite on the mucilage, which is found between the lateral branches. Some recent taxa are characterized by intracellular calcification of reproductive organs (cysts; Berger and Kaever, 1992). Fossil remains of dasycladalean algae are generally preserved as a mosaic of equant low-Mg calcite, but an original aragonitic mineralogy is inferred, based on the mineralogy of living representatives (Berger and Kaever, 1992) and diagenetic fabrics. A few species are known to have produced skeletons of low-Mg calcite (see review in Granier, 2012), but this character is generally not given supra-specific rank. Most of these originally calcitic species, which often show mass occurrences such as *Clypeina sulcata* and *Salpingoporella dinarica*, occurred in the latest Jurassic–Early Cretaceous, which was a time of 'calcite seas' (Stanley, 2008). However, in this same time interval, aragonitic dasycladaleans were diverse and abundant, which complicates the interpretation of the occurrence of calcitic species. Aguirre and Riding (2005) concluded that changes in dasycladalean diversity over the past 350 myrs show no straightforward relations with calcite- and aragonite sea intervals, while they broadly reflect global temperature and sea-level change. Dasycladales were prolific carbonate producers in Early Cretaceous carbonate platforms even if they did not attain the role of hypercalcifiers as in the Triassic (Stanley and Hardie, 1998). Nowadays, they have been largely substituted by Bryopsidales of the genus *Halimeda* as major carbonate producers in subtropical shallow-water realms (Granier, 2012).

4.2.4. Larger benthic foraminifers (LBFs)

LBFs are an informal group characterized by large size (from 0.1 to 15 cm) and complex internal structures (Ross, 1974; BouDagher-Fadel, 2018). They are single-celled eukaryotic protozoans with an epifaunal, motile or sessile life style. Living representatives are photosymbiotic but occasionally feed from microalgae and bacteria (Lee, 2006). Photosymbiosis is inferred for fossil taxa, mainly based on their large size and complex internal structures (Hottinger, 1982; Hallock, 1985; Lee and Hallock, 1987). Composition and microstructure of the test are generally used as the highest-rank character in the taxonomy of foraminifers (Sen Gupta, 2003), although more recently this approach has been partly questioned, based on the results of molecular phylogeny (Pawlowski et al., 2013; Dubicka, 2019). Recent photosymbiotic LBFs are found in two orders (Sen Gupta, 2003): Rotaliida, characterized by a hyaline test of lamellar low- or variable Mg calcite (Raja et al., 2005), and Miliolida, characterized by a porcelaneous test of high-Mg calcite. In Miliolida, the main body of the wall consists of needle-shaped crystallites, formed in the Golgi-vesicle and then transported to the outside of the test where they are coated by an external layer of round nanograins, seemingly formed by an organic membrane (Debenay et al., 2000; Parker, 2017; Dubicka et al., 2018). In Rotaliida, calcification occurs by crystal nucleation on an organic membrane, followed by addition of calcite on both sides of the membrane (Erez, 2003; De Nooijer et al., 2014).

Cretaceous LBFs feature a much larger variety of test mineralogy and microstructure than recent representatives. In addition to Miliolida (i.e., alveolinids and rhapydioninids) and Rotaliida (i.e., orbitoids and siderolitids), there are the Involutinida (i.e., trocholinids), secreting aragonitic tests, and Spirillinida (i.e., *Neotrocholina* and allied forms) secreting non-lamellar tests of calcite. In agglutinated groups, tests are made of sedimentary particles cemented by secreted calcite (Textulariida, i.e., orbitolinids and cuneolinids), or embedded in a proteinaceous to mineralized matrix (Lituolida, i.e., cyclamminids and choffatellids).

Studies on recent benthic foraminifers indicate that Rotaliida and Miliolida exert a strong control on biomineralization by enhancing *p*H and regulating ion concentration at the site of calcification (Debenay et al., 2000; de Nooijer et al., 2009). This conclusion can be confidently extended by analogy to Cretaceous miliolid and rotaliid larger foraminifers. A strong control on biomineralization can be hypothesized also for Cretaceous involutinids and spirillinids, based on their ability to control the mineralogy of their secreted test. A low level of control on biomineralization can be envisaged for agglutinating foraminifers, even, if for some species of Textulariida, the secretion of calcite cementing the grains could indicate a more direct control. Further indications can be gained by experiments of biomineralization under controlled conditions in laboratory and mesocosm experiments, and by field observations along natural CO_2 gradients. Most laboratory experiments reported a decrease of calcification at higher pCO_2 and lower *p*H in soritid porcelaneous larger benthic foraminifers, while studies on hyaline rotaliid species reported a variety of different responses, ranging from no change to increased calcification (Doo et al., 2014). More recently, decreased calcification rate under low *p*H was demonstrated for the hyaline larger foraminifer *Operculina ammonoides* (Oron et al., 2020). Field studies around natural CO_2 seeps reported steep reduction in density and diversity of calcifying foraminifers, compared with a less steep reduction of agglutinating taxa (Dias et al., 2010; Uthicke et al., 2013).

LBFs were abundant and diverse in the Cretaceous. Several groups attained rock-forming significance, including for instance the orbitolinids, alveolinids and orbitoids (van Gorsel, 1978; Vilas et al., 1995; Schroeder and Neumann, 1985). Recent LBFs can produce up to 2.8 kg $CaCO_3$ m^{-2} $year^{-1}$ in modern reefal environments (Hallock, 1981). They contribute about 5% to modern reefal carbonate production, and are considered as the third most important group of carbonate producers in modern coral reefs, after corals and red algae (Hallock, 1981; Narayan et al., 2022).

4.2.5. Corals

Recent zooxanthellate corals are attached, epifaunal, photosymbiotic, and feed on pico- and nannoplankton. Calcification is extracellular, with intermediate biological control but physiological control of the extracellular calcifying medium (Allemand et al., 2004; Wang et al., 2021). Scleractinian corals survive low-*p*H conditions and decalcification (Fine and Tchernov, 2007), and have a continuous phylogeny despite several 'reef gaps' in the geological record. Therefore, a calcareous skeleton may not be a requirement for phylogenetic survival. Their skeleton typically consists of aragonite, with very few exceptions (Stolarski et al., 2007). Diverse taxa such as *Acropora* have shown to be unaffected by changes in seawater chemistry for the last 40 myrs (Stolarski et al., 2016).

Carbonate production in modern coral reefs ranges from 1 to 35 kg m^{-2} a^{-1} (Barnes and Chalker, 1990), but <2.0 kg m^{-2} a^{-1} appears to be characteristic for most coral reef environments (Heiss, 1995). Azooxanthellate corals are predominantly solitary and small in size (rarely exceeding 20 mm in diameter; Cairns and Kitahara, 2012) and do not considerably contribute to carbonate production compared to zooxanthellate corals.

4.2.6. Rudist bivalves

Rudists lived as attached, epifaunal suspension feeders, but are not considered reef-builders because of the absence of growth fabrics that extended significantly above the sediment surface (Gili et al., 1995). Very few genera may have been photosymbiotic (Gili and Götz, 2018). As in modern bivalves, biological control of calcification was strong, and aragonite and low-Mg were precipitated from an extrapallial fluid,

isolated from seawater. The composition of the extrapallial fluid is controlled physiologically, to form multi-layered shells, protected by a chitinous periostracum. All rudists had inner shell layers composed of aragonite, including the myocardinal elements, and an outer shell layer of calcite with variable thickness and structures (Skelton and Smith, 2000). Rudists have been grouped into taxa that are aragonite-dominated, calcite dominated, or show no distinct dominance of one polymorph (Steuber, 2002; Steuber et al., 2016). Various shell structures developed among the rudist, and are related to palaeoecological morphotypes and feeding habits. The functional morphology of many of these shell structures is still debated (for details, see Gili and Götz, 2018; Skelton, 2018). The average stratigraphic range of genera of rudist bivalves is 8.5 myrs, and aragonite-dominated genera have significantly shorter average ranges (6.4 myrs) than calcite-dominated genera (10.8 myrs; Steuber et al., 2016).

Skeletal growth rates of rudist bivalves amounted to several cm/year (Steuber, 1996; Steuber et al., 1998; Steuber et al., 2005). Carbonate production by rudist bivalves has been estimated from skeletal growth rates and found to be up to 28.5 kg $CaCO_3$ m^{-2} $year^{-1}$ in dense growth fabrics (Steuber, 2000), well within the range of modern coral reefs.

4.3. Chalks

Significant deposition of pelagic carbonate began in the Jurassic, and the large-scale pelagic rain of carbonate into the deep sea, both in the form of tests of planktonic foraminifers and skeletal elements of calcareous nannoplankton, has continued ever since the Early Cretaceous (Hay, 2004; Suchéras-Marx et al., 2019). The global Albian–Cenomanian sea-level rise caused the flooding of vast epicontinental areas and a collapse of the shelf front. In combination with greenhouse conditions and high atmospheric CO_2 (Fig. 9), extensive, warm seas prevailed over large epicontinental areas. Hemi-pelagic conditions with water depths of a few hundred meters characterized the Western Interior Seaway, North Africa and large parts of Europe. These areas were characterized by a unique constellation in Earth history: a low input of siliciclastics resulted in the deposition of pure carbonates, the chalks. Chalks are here defined as biomicrites having a $CaCO_3$ content of 90–100%, a particle size of <20 μm, and significant porosity. The main components are calcareous nannofossils, calcispheres and planktonic foraminifers (in descending order). Earliest chalk deposits, up to 20 m thick, are known from the Barremian of the southern North-Sea area. Throughout the Cenomanian–Maastrichtian, chalks form an up to 1000 km wide facies belt between latitudes of c. 37°–50° N. This chalk belt extends from west of Ireland to the Caspian Sea in the east. In the southern North Sea, the Chalk Group, which includes the Danian, is up to 1500 m thick (Vejbæk et al., 2010). It reaches maximum thicknesses of >1500 m in the Central Graben of the North Sea and > 2000 m in the northern North Sea (Surlyk et al., 2003). Chalk is also documented from the Santonian–Maastrichtian of the US Gulf Coast region (Austin Chalk, max. 270 m thick), from the Western Interior (Niobrara Chalk, Coniacian–Campanian, max. 200 m thick; Selma Chalk, Santonian–Maastrichtian, max. 400 m thick), from Egypt and the Near East (Coniacian–Maastrichtian, max. 130 m thick) and Western Australia (Miria Chalk, Maastrichtian, 2 m thick). OAE2 coincided with reduced carbonate accumulation in epicontinental seas, and in pelagic environments (Uličný et al., 1993; Paul and Mitchell, 1994; Voigt, 2000).

A comparison of Late Cretaceous calcareous nannofossils from contemporaneous near-shore marls and off-shore chalks provides a differentiated view of their diversity and abundance patterns (Püttmann and Mutterlose, 2021). Highly diverse assemblages characterize the shallow-marine nearshore setting (0–10 km off the coast, about 10–40 m water depth). Diversities in the coastal area (species richness 50–81) are significantly higher than those of the contemporaneous chalk facies (species richness 43–53). At the same time, the abundances of the nearshore assemblages are by a factor of 2–10 lower than those of the chalk deposits. The "ecological deserts" of the chalk sea were thus dominated by a few *r*-selected opportunistic species. The high diversity assemblages of the nearshore setting occur in strongly glauconitic, marly–chalky intervals, likely resulting from elevated nutrient supply (Püttmann and Mutterlose, 2021).

4.4. Sea-level change and global carbonate sedimentation

Trends in generic diversity of calcareous nannofossils, planktonic foraminifers, and corals trace first-order Cretaceous sea-level change (Figs. 7, 8). Relatively short episodes of high sea level, (i.e., the Hauterivian), are also characterized by slightly higher numbers of genera of calcareous nannofossils and calcispheres. This is a common pattern (species-area effect, e.g., Hannisdal and Peters, 2011; Close et al., 2020), observed also in long-term Phanerozoic datasets of marine diversity, as it reflects marine sediment extent as a proxy for potential habitat area. The high Cretaceous sea level and extended epicontinental seas of the Late Cretaceous, in combination with high temperatures in intermediate and high latitudes, provided environments for geographic range expansion of carbonate-producing biota. Notably, the widespread distribution of chalks initiated during the peak Cretaceous sea-level in the Cenomanian (Fig. 7).

Pohl et al. (2020) compiled long-term neritic carbonate-preservation rates for the Cretaceous (Fig. 9d). These correspond well with empirical data (Bosscher and Schlager, 1993; Kiessling et al., 2000), which all provide a low-resolution envelope with a broad maximum in the Aptian–Cenomanian for the more detailed, albeit qualitative record (Fig. 9b, c) of Skelton (2003). Pohl et al. (2019, 2020), using climate-carbon cycle and palaeoecological niche models to understand the drivers of the observed trends, concluded that continental configuration, including eustatic sea level, and volcanic degassing controlled first-order variations in Cretaceous neritic carbonate sedimentation (Fig. 9e). The models of Pohl et al. (2020), which address carbonate sedimentation on the order of 10 myrs, do not account for large igneous provinces, the presumed causes of OAEs, because the CO_2 degassing by LIPS was short-term, on the time scale of a few myrs. These models only considered extrinsic factors and explicitly excluded changing biota with different carbonate-production rates. Dutkiewicz et al. (2019) reconstructed neritic carbonate-accumulation fluxes using the extent of carbonate platforms (Kiessling et al., 2003; Fig. 9e), and preservation rates of Bosscher and Schlager (1993). They suggested a different temporal pattern, with highest rates in the Late Cretaceous and a late Campanian–Maastrichtian maximum. These discrepancies highlight the problem of estimating such depositional fluxes. The quantitative and qualitative estimates compiled here (Fig. 9b–e) provide the background for the discussion of our palaeobiological data. Overall, estimates of carbonate accumulation and preservation rates track sea level and flooded continental areas (Fig. 9e), as compiled by Cao et al. (2017).

4.5. Oceanic anoxic events

Except for the calcareous nannofossils, calcispheres, and planktonic foraminifers, all other groups of biocalcifiers considered here show significant reductions in diversity during or before the two main Cretaceous OAEs (i.e., the early Aptian OAE1a and the late Cenomanian OAE2). The Valanginian Weissert event affected dasycladaleans and rudist bivalves, but not LBFs and corals. Leckie et al. (2002) demonstrated elevated rates of turnover (extinction and speciation) in the planktonic foraminifers, and to a lesser extent the calcareous nannofossils, associated with the mid-Cretaceous OAEs, particularly OAE1a, 1b, and OAE2.

Increasing evidence indicates that OAE1a and OAE2 were caused by intensive submarine volcanism of large igneous provinces (Matsumoto et al., 2022), and followed similar sequences of events. An initial rise in atmospheric CO_2 concentrations during episodes of increased volcanism, with the possible contribution of methane release in the case of OAE 1a (Erba, 2004; Weissert and Erba, 2004; Bodin et al., 2015; Adloff

et al., 2020), resulted in climate warming and possibly reduction of sea-surface carbonate saturation. This was followed by increased continental weathering, increased nutrient and carbonate-ion fluxes to the oceans, resulting in increased marine production of organic matter. High organic carbon burial may have been additionally facilitated by high seawater temperature due to the CO_2 greenhouse effect of LIP volcanism. The case is less clear for the Weissert event, for which a similar sequence of events and relation to volcanic CO_2 injection has not yet been unequivocally established (Föllmi, 2012; Price et al., 2018; Cavalheiro et al., 2021). Despite these unknowns, all three events represent short-term perturbations of variables of the atmosphere-ocean system that may have affected carbonate producers: sea-surface carbonate saturation, temperature, and nutrient fluxes. These variables are discussed here in separate sections. Oceanic anoxia occurred in basinal intermediate and deeper waters, but there is no clear evidence for anoxic sea-surface water to have affected carbonate platforms.

OAE1a and OAE2, which are both documented in many sites by TOC-rich black-shale intervals, are also characterized by a reduction of pelagic biogenic carbonate production. In calcareous nannofossils, significant declines of the heavily calcified nannoconids, a group of nannoliths, have been observed directly pre-dating the Weissert and the OAE1a events (nannoconid crisis; Erba, 1994; Erba et al., 2010), and the latest Aptian OAE1b (Leckie et al., 2002; Huber and Leckie, 2011). However, OAE1a is preceded by a major speciation event, and does not show significant extinctions of calcareous nannnofossils. The increase of nutrients and atmospheric CO_2 across the OAEs possibly induced higher abundances of shallow-dwelling heterococcoliths, which produced small forms outcompeting the deep-dwelling nannoconids (Erba, 2004).

For an evaluation of the effects of environmental change related to OAEs on carbonate producers, the precise timing of taxon originations and extinctions is important, which is beyond the stratigraphic resolution of the current study. During the early Aptian most subtropical carbonate platforms and their biota disappeared during, or shortly before, the negative carbon-isotope excursion (CIE) at the onset of OAE1a that reflects the injection of large amounts of CO_2 into the ocean-atmosphere system (Skelton, 2003). In lower latitudes, carbonate platforms persisted and many rudist genera that previously disappeared from higher latitudes survived the anoxic event and its positive CIE. These taxa finally became extinct at the end of the early Aptian, possibly related to a major sea-level fall (Strohmenger et al., 2010; Skelton and Gili, 2012). In our dataset, the affected rudist genera range to the top of the lower Aptian. However, the environmental perturbations of OAE1a caused a significant latitudinal range reduction in the palaeogeographic distribution of rudists already in the earliest Aptian, during the initial volcanic pulse that is believed to have initiated the OAE. Detailed patterns of extinction have also been found in LBFs across OAE2 (Parente et al., 2008), explained with changes in nutrient cycling, and correlated to other environmental perturbations during the first phase of OAE2. The recognition of such patterns on a high-resolution scale is important to disentangle the cause-effect relationships of the various aspects of environmental change related to Cretaceous OAEs that are discussed in the following sections.

4.6. Sea-surface temperature

Cretaceous sea-surface temperatures (Fig. 9f) have been reconstructed from organic geochemical proxies (Tex_{86}), and stable oxygen isotope values of planktonic foraminifers (O'Brien et al., 2017). Except for a currently not well-defined drop in the Albian, high temperatures prevailed until the Turonian, with a subsequent decrease until the end of the Cretaceous. A short-lived maximum is evident in Tex_{86} data for OAE1a, while the late Cenomanian and Turonian peak was more long-lived (Forster et al., 2007; Friedrich et al., 2012; Huber et al., 2018). Considering the short-term, but significant CO_2 increase at the onset of Cretaceous OAEs, and the low resolution of geological records, the temperature increase during such events is most likely underestimated (Kemp et al., 2015).

In the fossil record, turnovers frequently coincide with hyperthermals (Foster et al., 2018; Reddin et al., 2021). Hyperthermals, including those of the early Aptian and Cenomanian/Turonian transition, affected photosymbiotic and aragonitic biota significantly (Reddin et al., 2021). This is also reflected in our data for the LBFs, rudists, and dasycladalean algae, and to a lesser extent in the total number of coral genera. For the photosymbiotic Scleractinia, high temperatures may have disrupted photosymbiosis, in analogy with current climate change, although some modern Scleractinia have shown to adapt to high temperatures (Hume et al., 2016). A mid-Cretaceous episode of a likely loss of photosymbiosis in corals was proposed by Kiessling and Kocsis (2015), based on a dataset with a stage-level stratigraphical resolution. This agrees with a marked rise in the fraction of azooxanthellate genera of all coral genera in the late Aptian (i.e., after OAE1a; Fig. 10). Following OAE2, the rise in the proportion of azooxanthellate genera is only minor. Substantial increases in the relative number of azooxanthellate genera occurred in the Campanian and Maastrichtian, when temperature and pCO_2 dropped. Disruption of photosymbiosis and demise of zooxanthellate genera due to high temperatures thus may have occurred in the context of OAE1a. The significant rise in the relative number of azooxanthellate genera in the Campanian–Maastrichtian, however, requires a different explanation.

Among the other groups considered here, the negative effect of high temperature on photosymbiosis may apply to the LBFs. This is most evident for OAE2, when all groups show significant declines, and aragonitic hyaline taxa disappeared.

Global warming, which is related to the majority of extinction events throughout Earth's history (Harnik et al., 2012), may be the result of perturbation of the carbon cycle that triggered ocean acidification and oceanic anoxia. However, it remains elusive, if such warming events had been the trigger, or an outcome of other factors of environmental change that caused mass extinctions. Harvey et al. (2013) have shown that seawater warming and acidification together increase stress on modern marine calcifiers, but affect taxa differently. Detrimental effects of high temperatures combined with ocean acidification have also been documented for recent LBFs (Schmidt et al., 2014; Kenigsberg et al., 2022).

4.7. Nutrients

Phosphorous is an important nutrient for all organisms, and its availability limits primary production in large parts of the ocean (Paytan and McLaughlin, 2007). Unlike nitrogen, another limiting nutrient for marine primary production that can be fixed from the atmosphere, the only significant source of phosphorous to the ocean is from continental weathering. In the modern ocean, the supply of new, weathering-derived phosphorous (i.e., from riverine and atmospheric sources), is negligible. It amounts to $<0.5\%$ of the ocean internal cycling within the photic zone and by upwelling (Schlesinger and Bernhardt, 2020). Therefore, phosphorous is considered to be the ultimate limiting nutrient for marine ecosystems (Paytan and McLaughlin, 2007), and we focus our discussion on available data for phosphorous accumulation rates in marine sediments (Föllmi, 1995) as a proxy for nutrient fluxes during the Cretaceous.

As the residence time of phosphorous in seawater is relatively short (20,000–100,000 years; Paytan and McLaughlin, 2007), the availability of nutrients in sea-surface waters depends on ocean circulation (e.g., upwelling), local riverine input and atmospheric deposition. Therefore, regional rather than global patterns are to be expected. Furthermore, low oxygen concentration in deep water can promote release of phosphorous from sediments, which may result in a self-sustaining mechanism of anoxic conditions (Watson et al., 2017), but this effect on the long-term, internal phosphorous cycling of the ocean is controversial (Beil et al., 2020).

The availability of nutrients had different effects on the different groups of carbonate producers discussed here, characterized by

heterotrophic, autotrophic, and mixotrophic autecology. Mixotrophic organism, i.e., those with a combined heterotrophic and photosymbiotic autecology such as corals and LBFs, have significant advantages in the photic zone of oligotrophic environments (Hallock, 1981, 2001). In such biota, ingested food provides nutrients, while energy is sourced from carbohydrates provided by symbiotic algae (Pomar and Hallock, 2008).

The role of nutrients in modern carbonate-producing marine environments is well established (e.g., Hallock and Schlager, 1986), and reflected in marine biodiversity gradients (Hallock, 1987). Elevated nutrient fluxes have been invoked to explain episodes of carbonate-platform drowning in the geological record. Nutrients support primary production so that heterotrophic organisms are able to outcompete the frequently phototrophic prime carbonate producers (Hallock and Schlager, 1986). This hypothesis is based on observations of modern carbonate-depositional systems. Its application to the geological record assumes that major carbonate-producing ecosystems of the past relied on photosymbiosis and thus required oligotrophic environments (see overview of classifications of neritic carbonates and nutrient levels in Mutti and Hallock, 2003). However, symbionts of modern zooxanthellate corals may have only originated in the Eocene (Pochon et al., 2006), and the coexistence of corals, rudists, sponges, stromatoporoids and microbes on Cretaceous carbonate platforms questions the uniformitarian paradigm of oligotrophy for corals, and carbonate-producing ecosystems in general (Pomar and Hallock, 2008). Zooxanthellate coral assemblages thriving in low-light and nutrient-rich environments have been reported from, for example, the late Aptian, post-OAE1a deposits (Tomás et al., 2008).

Despite very limited, circumstantial evidence for photosymbiosis in rudist bivalves (Gili and Götz, 2018), these characteristic Cretaceous bivalves are frequently considered to belong to the photozoan group of carbonate producers, with the implicit similarity to modern coral reefs and their environmental preferences (Föllmi, 2012; Föllmi and Godet, 2013). In view of these uncertainties, phototrophic communities may not have been the most prolific carbonate producers in the Cretaceous, and heavily calcified rudist bivalves as epifaunal suspension feeders must instead be assumed to have benefitted from elevated nutrient fluxes. Even if nutrients may have adversely affected oligotrophic skeletal carbonate production on carbonate platforms, microbial or non-skeletal carbonates may have become more abundant (Smith et al., 2021), as postulated for *Bacinella*-rich carbonates during OAE1a (e.g., Rameil et al., 2010; Huck et al., 2012).

Intuitively, autotrophic and heterotrophic planktonic organisms are expected to benefit from high nutrient availability. However, eutrophic environments are typically unstable, and the greater depth of the euphotic zone in oligotrophic pelagic environments promotes diversification of planktonic carbonate producers along large, depth-related environmental gradients (Hallock, 1987). Coccolithophores were found to be more diverse but less abundant in Late Cretaceous mesotrophic to temporarily eutrophic nearshore settings when compared to oligotrophic to temporarily mesotrophic, hemipelagic chalk environments (Püttmann and Mutterlose, 2021). This highlights the observation that diversity is a weak indicator of carbonate-production potential, as low-diversity assemblages - or even a single species - may locally or regionally act as important carbonate factories (Pomar and Hallock, 2008). Nevertheless, a high diversity of specific groups of organisms indicates favourable environmental conditions for the exploitation of ecological niches, which will result in the evolution of taxa that may thrive as major carbonate producers elsewhere. In this context, high phosphorous accumulation rates in the Late Cretaceous (Fig. 7), coincide with a high diversity of nannofossils and planktonic foraminifers. These in turn go along with widespread chalk deposition, and the highest diversity of rudist bivalves and LBFs.

Elevated nutrient fluxes to the ocean as a result of increased continental weathering and an accelerated hydrological cycle due to global warming are considered an important mechanism that resulted in Cretaceous OAEs. In the compilation of phosphorous fluxes into marine sediments (Föllmi, 1995), a minor peak coincides with OAE1a, but no elevated flux coincides with OAE2 (Fig. 7). Due to the short residence time of phosphorous in seawater, short-term peaks in phosphorous fluxes during OAEs may not be reflected in the compilation of Föllmi

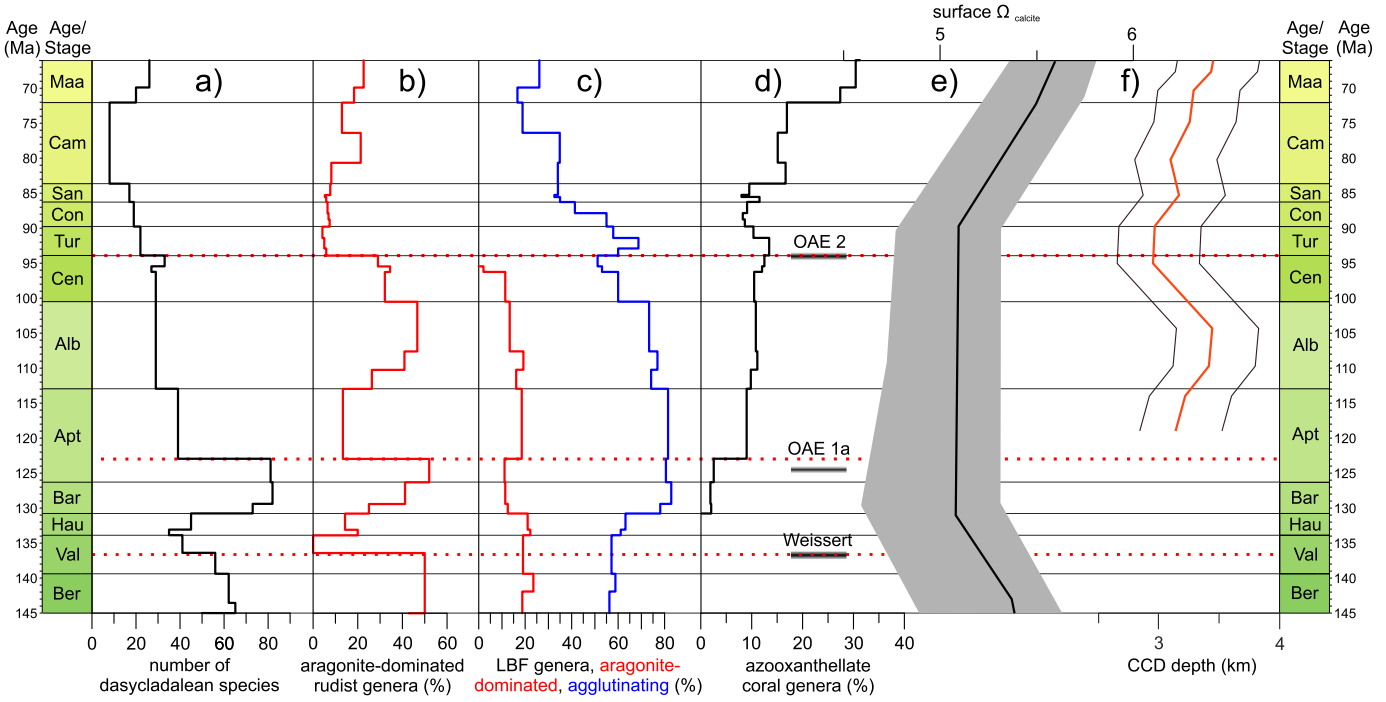

Fig. 10. Numbers of dasycladalean species (a); percentage of genera of rudist bivalves with aragonite-dominated shells (b); percentage of genera of aragonitic and agglutinating-microgranular larger benthic foraminifers (c); percentage of azooxanthellate coral genera (d); modelled surface-water calcite saturation (e, Ridgwell, 2005); depth of calcite compensation depth (f, Dutkiewicz et al., 2019). Red dashed horizontal lines indicate extinction events. (For interpretation of the references to colour in this figure legend, the reader is referred to the web version of this article.)

(1995), although these may have caused regional platform drowning. Increased fluxes of phosphorous to the ocean by enhanced continental weathering and seawater interaction with hot LIP basalts is implicated by geochemical proxies for OAE1a (e.g., Lechler et al., 2015) and OAE2 (e.g., Yobo et al., 2021). For OAE1a, the demise of carbonate platforms coincided with or preceded the initial negative CIE. The onset of volcanism was followed by increased nutrient fluxes and organic carbon burial, at a time when carbonate platforms had already retreated to low palaeolatitudes, and 'out-of-balance' microbial carbonate producers were abundant (e.g., Rameil et al., 2010; Amodio and Weissert, 2017). The demise of carbonate platforms during OAE2 and their characteristic carbonate producers such as rudists and LBFs appears to coincide with the onset of the positive CIE (Philip and Airaud-Crumiere, 1991; Voigt, 2000). The extinction pattern of LBFs during this phase has been interpreted to reflect an increasing nutrient flux (Parente et al., 2008). However, the evolution of carbonate platforms during OAE2 appears not to be linked to palaeolatitude (e.g., Philip et al., 1995; Drzewiecki and Simo, 2000; Parente et al., 2008; Korbar et al., 2012; Navarro-Ramirez et al., 2017).

Pohl et al. (2019) found a better match for the occurrence of Aptian carbonate platforms in a low-productivity biogeochemical model scenario than in high-productivity model runs. Upwelling zones modelled for the north African continental margin during the Late Cretaceous (Hay, 2009) coincide with the near absence of rudists and corals from this palaeogeographic domain (Steuber and Löser, 2000). There is also a remarkable match in the predicted distribution of low-latitude sites of upwelling (Hay, 2009) and the absence of carbonate platforms in the Early Cretaceous (Pohl et al., 2019). Our current database, however, does not allow for a detailed evaluation of regional patterns of nutrient fluxes and their contribution to the demise of neritic carbonate production.

In summary, the effect of nutrient fluxes on carbonate production remains difficult to evaluate. Due to biochemical constraints and the short residence time of important nutrients in seawater, regional patterns most likely controlled nutrient fluxes as a function of continental weathering, volcanic input, and oceanic circulation. A comparison with secular trends in the global distribution in the diversity of major carbonate producers is therefore not feasible. Another problem is the unknown autecology of many Cretaceous taxa, and the extent to which modern ecological patterns in the distribution of carbonate producers can be extrapolated to the Cretaceous. In addition, diversity is not necessarily connected to reef building capacity. Likewise, high diversity and photosymbiosis do not translate into significant carbonate production, if seawater chemistry and other environmental factors are not adequate. However, there is a coincidence of Late Cretaceous chalk deposits in the northern hemisphere with globally high phosphorous accumulation rates (Fig. 7). The predicted upwelling zones in low–mid latitudes are in regions from which major carbonate platforms are absent in the Early and Late Cretaceous.

4.8. Seawater chemistry

4.8.1. CO_2, pH, and the seawater carbonate system

The mid-Mesozoic expansion of pelagic carbonate producers that shifted the dominant areas for carbonate deposition from the continental shelves to the open ocean introduced a buffering mechanism for the global biogeochemical cycling of calcium carbonate through the dynamics of the lysocline (Ridgwell, 2005). Therefore, the Cretaceous–Recent oceans were much better buffered against extreme changes in carbonate saturation than those of the earlier Phanerozoic, when carbonate deposition was largely restricted to continental shelves (Ridgwell, 2005). Evaluation of past carbonate-seawater chemistry is difficult, considering uncertainties of past major ion concentrations and chemical equilibrium constants (Hain et al., 2015; Zeebe and Tyrrell, 2018, 2019). A multitude of papers has focused on the effect of rising atmospheric pCO_2, decreasing sea-surface pH ('ocean acidification'), and of related changes in the marine carbonate system on marine calcifiers (e.g., Ries et al., 2009; Leung et al., 2022). In various groups of organisms, adverse effects such as reduced calcification, shell dissolution, altered shell structures, changes in carbonate mineralogy, and other biological effects have been identified (Cameron et al., 2019). Such effects, however, are not uniform, even between related genera, and are assumed to relate to different calcification pathways (e.g., de Nooijer et al., 2009).

The decrease in carbonate-ion concentration triggered by the rapid injection of massive amounts of volcanogenic CO_2 at the onset of OAEs probably inhibited biocalcification in calcareous nannofossils (Erba, 1994, 2004, 2006; Riebesell et al., 2000) and planktonic foraminifers (Barker and Elderfield, 2002; Leckie et al., 2002; Huber and Leckie, 2011). The size decrease of calcareous nannofossils during the nannoconid crisis at the onset of OAE1a may then be interpreted as a dissolution event, related to the LIP volcanic CO_2 release, methane release, and changes in ocean water chemistry, or as a result of eutrophication (Erba et al., 2010). High-resolution sedimentary and geochemical records from a low-latitude carbonate-ramp depositional system also show a short-lived dissolution event coinciding with the peak negative CIE of OAE1a (Steuber et al., 2022). The absence of a negative CIE near the base of the OAE2 suggests a volcanic CO_2 source without methane release. In this case the substantial input of volcanic CO_2 is seen as the major factor limiting the calcification process of calcareous nannofossils.

It is important to note that a reduction in pH values and elevated atmospheric pCO_2 will only result in a reduction of carbonate saturation of seawater if injection of CO_2 occurs on time scales short enough to prevent the dynamics of the lysocline to maintain carbonate saturation (i.e., during less than c. 50 kyr; Zeebe, 2001; Hönisch et al., 2012). On longer time scales, low pH caused by elevated atmospheric CO_2 is not necessarily linked to reduced carbonate saturation because increases in atmospheric CO_2 result in an increase in total alkalinity. Geochemical modelling based on carbon and osmium isotope data for OAE1a has shown that a short-lived (50 kyr) increase of volcanic CO_2 emission by a factor of 6–10 will cause measurable acidification-related results, but not carbonate undersaturation (Bauer et al., 2017). Such events of the reduction of both, pH and carbonate saturation, have been discussed for OAE1a and OAE2, but the relevant geological evidence is still controversially discussed (Erba et al., 2010; Gibbs et al., 2011; Hönisch et al., 2012; Steuber et al., 2022). Comparatively high seawater Ca^{2+} concentration of Cretaceous seawater will also have contributed to buffer carbonate saturation, as a relatively low carbonate-ion concentration is required to maintain saturation (Demicco et al., 2005; Hönisch et al., 2012).

Aragonite saturation requires a higher solubility product than calcite saturation, and saturation typically decreases with temperature and thus latitude (Opdyke and Wilkinson, 1990). This may explain why the numbers of genera of most aragonitic or aragonite-dominated carbonate producers where decimated at OAE1a and OAE2, and carbonate platforms retreated to lower latitudes at the onset of OAE1a (Strohmenger et al., 2010; Skelton and Gili, 2012).

A comparison of the percentage of aragonitic or aragonite-dominated genera of rudist bivalves, LBFs, and the number of genera and species of dasycladalean algae shows remarkably similar patterns of an overall decrease from the Early to the Late Cretaceous, punctuated by significant decreases during OAE1a and OAE2 (Fig. 10). Compared with model reconstructions of long-term sea-surface carbonate saturation (Ridgwell, 2005) and atmospheric pCO_2 (Foster et al., 2017, 2018), aragonite precipitation was more physiologically costly during the mid-Cretaceous period of high atmospheric pCO_2 and reduced sea-surface carbonate saturation, so that short lived, possibly more extreme reductions of carbonate saturation at the onset of OAEs (Bauer et al., 2017), caused extinction events among several groups of aragonitic carbonate producers. For OAE2, the rise of the CCD (Fig. 10) at the Cenomanian–Turonian transition is also in line with a reduction in seawater

carbonate saturation. Such data are not available for OAE1a, but there is evidence for a shallowing of the CCD in the early Aptian (Thierstein, 1979; Wohlwend et al., 2017).

In contrast to aragonitic carbonate producers, the percentage of agglutinating and microgranular foraminifers peaked during the Barremian–Cenomanian. Orbitolinids, for example, globally characterize carbonate-platform systems at the onset of OAE1a (Amodio and Weissert, 2017). Culture experiments (Dong et al., 2020) and studies in natural environments (Dias et al., 2010) have shown that among modern benthic foraminifers, those with agglutinating tests are not negatively affected or even increase in test size with decreasing *p*H values of seawater. It therefore seems plausible to assume that aragonitic or aragonite dominated rudist bivalves, LBFs, and dasycladalean algae were affected by changes in the marine carbonate system during the mid-Cretaceous, which culminated in crises of carbonate saturation during OAE1a and OAE2. Cretaceous corals were affected during OAE2, but show only limited reductions in the number of genera during OAE1a.

According to the sequence of events that caused OAE1a and OAE2, global warming and elevated atmospheric pCO_2 amplified the hydrologic cycle, thereby increased continental weathering, and resulted in an alkalinity overshoot immediately following a short-lived episode of reduced seawater carbonate saturation (e.g., Penman et al., 2016; Smith et al., 2021). Evidence for such overshoots may be recorded in the Ca-isotopic composition of marine carbonates (Fantle and Ridgwell, 2020), but should also be recorded in the geological record. Carbonate platforms and carbonate producers recovered slowly, on much longer time scale than an alleged alkalinity overshoot. Circumstantial evidence for an alkalinity overshoot may be found in thick oolites that follow over the deposits of OAE1a on Pacific guyots (Jenkyns and Wilson, 1999), in the rapid aggradation of low-latitude carbonate platforms (Strohmenger et al., 2010), or possibly in the abundance of chalk deposition after OAE2.

4.8.2. Seawater Mg/Ca

Inorganic precipitation experiments have shown that the Mg/Ca ratio of seawater affects the precipitation of $CaCO_3$ polymorphs. A high Mg/Ca ratio favours the precipitation of aragonite and high-Mg calcite, while a low Mg/Ca favours the precipitation of low-Mg calcite (Morse et al., 1997). Geochemical modelling and proxy data have shown that during the Phanerozoic the Mg/Ca molar ratio of seawater has oscillated on times scales of c. 100 myrs between values of c. 1 and 5 (Stanley and Hardie, 1998; Lowenstein et al., 2001). This has resulted in the concept of calcite and aragonite seas, with the skeletal mineralogy of major carbonate producers generally matching these predicted long-term trends (Sandberg, 1983; Stanley and Hardie, 1998). However, there is no clear threshold between calcite and aragonite seas, considering the effect of other parameters that control carbonate saturation, particularly the latitudinal temperature gradient (Balthasar and Cusack, 2015). For Cretaceous rudist bivalves, patterns of aragonite versus calcite dominance have been reported previously (Steuber, 2002; Steuber et al., 2016). The observed pattern is too complex as to be explained merely by the seawater Mg/Ca ratio, which rose from low values of c. 1 during the Early Cretaceous to values of c. 2 during the Late Cretaceous, and continued to rise in the Cenozoic to the modern value of c. 5. As the seawater Mg/Ca ratio was generally low during the Cretaceous, the complete period was classified as a calcite sea (Stanley and Hardie, 1998).

The overall trend of decreasing aragonite versus calcite observed in the Cretaceous carbonate producers matches observations of van de Poel and Schlager (1994) on the bulk composition of skeletal carbonates. This general pattern is, in fact, opposite of what should be expected from inorganic precipitation experiments, as the proportion of aragonite-dominated taxa is highest during the Early Cretaceous period of low seawater Mg/Ca ratio, and declines with increasing Mg/Ca ratio during the Late Cretaceous. Because of the long residence time of Mg and Ca in seawater (c. 13 and c. 1 myrs, respectively, Broecker and Yu, 2011), the slowly changing ratio of these elements in seawater can only be considered as a baseline parameter. It cannot be invoked to have caused short-term pattern, such as the observed extinction events of aragonitic or aragonite-dominated taxa.

Kiessling et al. (2008) examined preference for skeletal mineralogy during the extinctions and recovery intervals of major Phanerozoic mass extinctions, and observed variable patterns of mineral dominance. These are, however, not consistent with the aragonite or calcite seas prevailing during the events (e.g., aragonite extinction and calcite recovery during calcite seas and vice versa). This lack of consistency argues for factors other than Mg/Ca that affect carbonate saturation. While long-term trends in skeletal mineralogy appear to reflect calcite and aragonite seas (Stanley and Hardie, 1998), mass extinctions shape the dominance more significantly, but with no clear relations of extinctions and originations to the seawater Mg/Ca ratio. Therefore, the direction of mineralogical change after mass extinction cannot be predicted by the prevailing seawater Mg/Ca ratio (Kiessling et al., 2008). The demise of aragonitic biota during the Cretaceous crises of carbonate platforms is similar to the pattern observed at the Triassic/Jurassic boundary (Hautmann, 2004), but opposite to the pattern at the Permian–Triassic boundary (Railsback and Anderson, 1987), although the latter two major extinction events occurred during an episode of similar seawater Mg/Ca ratios. Likewise, the Phanerozoic distribution of the few calcitic species of dasycladalean algae is not linked to the seawater Mg/Ca ratio (Granier, 2012).

Eichenseer et al. (2019) used Phanerozoic seawater Mg/Ca and surface temperature models to calculate 'aragonite sea intensity' (ASI), and found this index to correlate with the relative success of aragonitic versus calcitic genera for the Ordovician–Triassic, but not thereafter. This mismatch was attributed to the proliferation of calcareous plankton in the mid-Jurassic, which fundamentally altered the internal buffering of the carbonate system of the ocean (Ridgwell, 2005). In fact, according to Eichenseer et al. (2019), the aragonite sea intensity reached its lowest Phanerozoic value during the Early Cretaceous and rose to moderate values during the Late Cretaceous, which cannot explain the opposite trend observed in our dataset.

4.9. Contrasting response of diversity to environmental change

The flooding of continental areas and the expansion and demise of carbonate platforms are reflected in the diversity patterns of the carbonate-producing biota, similar to what has been identified as controls on marine biodiversity on Phanerozoic time scales (Close et al., 2020). However, the comparison of diversity patterns with aspects of environmental change that are considered important for carbonate precipitation, has revealed non-uniform and contrasting patterns. Corals, planktonic foraminifers, and calcareous nannofossils, groups with fundamentally different autecology, and precipitating different carbonate polymorphs (aragonite and calcite, respectively), show similar diversity patterns throughout the Cretaceous. Their distribution predominantly reflects first-order sea-level change, with corals showing variable reductions in the number of genera during carbonate platform crises related to OAEs. It therefore appears plausible to assume that the expansion of suitable habitats during episodes of high sea level and high temperatures were more important controls of diversity in these groups than changes in seawater chemistry. Compared to other calcareous biota, Eichenseer et al. (2019) found the least impact of 'aragonite sea intensity', calculated from seawater Mg/Ca ratio and palaeotemperature, on scleractinian corals.

All other taxa investigated show more complex trends, closely related to the waxing and waning of carbonate platforms, with a relatively uniform pattern of decreasing aragonite abundance with time, both in monomineralic and bi-mineralic taxa, and significant reductions in aragonitic genera numbers at OAEs. There is some coincidence with a mid-Cretaceous, relatively low seawater carbonate saturation and the overall trend of decreasing aragonite at that time (Fig. 10), but model

estimates of seawater carbonate saturation are only available at a low temporal resolution. Short-lived, more severe reductions in carbonate saturation may have occurred at the onset of OAEs (e.g., Bauer et al., 2017), caused by volcanic CO_2 emissions that are believed to have triggered OAEs. Such events, however, appear to have affected taxa with a high biological control of carbonate precipitation such as rudists to the same extent, or even more severely, as groups with a moderate or low biological control on calcification, such as the LBFs and dasycladalean algae.

4.10. Long-term versus short term effects

Our dataset reports the stratigraphic distribution of the taxa investigated at the substage level. Some of the proxies of environmental change discussed, such as variations in sea level, palaeotemperatures, and atmospheric pCO_2 are reconstructed at a similar or higher stratigraphic resolution. Other important proxies, particularly those affecting the seawater carbonate system, are only available at a much lower temporal resolution. This makes the evaluation of cause–effect relationships difficult. At the other extreme of relevant time scales (i.e., at the level of individual life spans) numerous culture experiments with artificial, modified seawater have shown variable effects on carbonate producers. Such experiments do not take into account the time scales of natural environmental change and the adaptive potential of calcifying biota. On Phanerozoic time-scales such effects have been addressed by normalization of available data, and some patterns appear to be evident, such as the concept of calcite and aragonite seas (Stanley and Hardie, 1998), the observation of global warming being related to the majority of extinction events (Harnik et al., 2012), or the effect of sealevel on marine biodiversity (Close et al., 2020).

An example of the time scales involved in such analyses are data and model-derived estimates of surface areas of carbonate platforms (Kiessling et al., 2003; Pohl et al., 2019), neritic carbonate-preservation rates (Pohl et al., 2020), which reflect flooded continental areas (Cao et al., 2017), and ultimately first-order Cretaceous sea level change (Figs. 7, 9). The temporal distribution of these data and model estimates reflects long-term environmental change during the Cretaceous. Their temporal resolution, however, is too low to aid in the identification of drivers of change in the observed diversity patterns of carbonate producers. Qualitative estimates of the extent of global carbonate platforms (Skelton, 2003) more closely resemble the temporal distribution of carbonate-platform dwelling biota, but may involve a sampling bias introduced by the stratigraphic records of Cretaceous carbonate platforms.

On time scales of 100 s of myrs, Scleractinia and particularly a photosymbiosis autecology exhibit a large 'relative hyperthermal vulnerability' (Reddin et al., 2021), while epifaunal and suspension feeding life habits had a lower vulnerability. This contrasts our data, while the observation that aragonite skeletal mineralogy appears to carry a larger hyperthermal extinction risk than low-Mg calcite, conforms with our observation. Such studies, however, cannot discern if high temperature was the functional mechanism, or a reflection of other perturbations of Earth systems, such as short-lived events of low seawater carbonate saturation due to pulses of volcanic CO_2 release, triggering OAEs. Considerable progress has been made recently to decipher the sequence of events of OAEs such as the timing, durations and amounts of CO_2 emission, global warming, and effects on the seawater carbonate system (e.g., Erba et al., 2010; Hönisch et al., 2012; Bauer et al., 2017; Kuhnt et al., 2017; Jenkyns, 2018; Beil et al., 2020; Castro et al., 2021; Matsumoto et al., 2022). These studies typically refer to hemipelagic deposits, where orbital chronology provides the time frame to evaluate, for example, relatively short-term perturbations of the carbon cycle that may have affected seawater-carbonate saturation. Such high-resolution studies are relatively rare in carbonate-platform deposits, where the distinct carbon-isotope pattern of OAEs typically provide the best tool for correlation. Unfortunately, this tool is frequently affected by diagenetic alterations (e.g., Parente et al., 2008; Huck et al., 2010; Strohmenger et al., 2010; Skelton and Gili, 2012; Amodio and Weissert, 2017; Steuber et al., 2022). Although the temporal record of carbonate platforms is rather fragmentary (Schmitt et al., 2020), particularly during episodes of OAEs, these archives are important to better understand the sequence of events that resulted in the diversity patterns of major carbonate producers, and more high-resolution studies across these intervals of crisis are required.

5. Conclusions

The compilation of the stratigraphic ranges of genera of important Cretaceous planktonic and benthic carbonate producers reveals two major, disjunct patterns in their evolution of diversity. Calcareous nannofossils, calcispheres, planktonic foraminifers, and corals trace sea level, flooded continental areas, and, to a lesser extent, neritic carbonate-preservation rates, while larger benthic foraminifers (LBFs), rudist bivalves, and dasycladalean algae trace the temporal distribution of carbonate platforms.

OAE1a and OAE2 are marked by pronounced extinction events of rudists, LBFs, and dasycladalean algae, affecting predominantly aragonitic taxa. Corals show a significant reduction in genera in the aftermath of OAE2, but only a minor reduction after OA1a. These extinction episodes are characterized by short-lived, major increases in atmospheric CO_2 and the highest Cretaceous sea-surface temperatures. As the autecology of rudists and LBFs relies significantly on calcification, the observed patterns may be explained by intermittent stress due to reduced carbonate saturation caused by spikes in atmospheric CO_2 concentrations sufficiently short to have escaped the internal buffering of seawater carbonate saturation by the dynamics of the lysocline. High sea-surface temperatures associated with volcanic CO_2 emissions may have disrupted photosymbiosis in corals and LBFs, but cannot explain the significant reduction in aragonite-dominated rudists. The relative number of azooxanthellate coral genera increases substantially after OAE1a, arguing for a disruption of photosymbiosis due to high temperatures, but the continuous increase in the relative number of genera of azooxanthellate corals in the Late Cretaceous cannot be explained with temperature stress.

Phosphorous accumulation in marine sediments is considered here as a proxy for nutrient availability. Due to the short residence time of phosphorous and other important nutrients, these may have affected carbonate producers regionally during times of increased continental weathering following relatively short-lived episodes of increased atmospheric pCO_2 that initiated OAEs. The absence of carbonate platforms from Cretaceous upwelling areas is noted, but the ecological response to nutrient availability of certain groups of Cretaceous carbonate producers cannot confidently be extrapolated from their modern relatives.

Higher carbonate saturation is required for aragonite precipitation than for calcite. This may explain the higher vulnerability of aragonitic taxa during Cretaceous extinction episodes, and the contraction of carbonate platforms to lower latitudes during OAE1a. There is a distinct long-term trend of decreasing aragonitic or aragonite-dominated taxa until the Campanian, which agrees with model simulations of seawater carbonate saturation. Such model simulations are, however, only available with a very low temporal resolution.

The Mg/Ca ratio of seawater is not considered to have contributed to the observed pattern, as it was relatively stable and low during most of the Cretaceous, with a slow rise in the Late Cretaceous. The Cretaceous is typically considered to be an episode of 'calcite seas', and the long-term trend of decreasing aragonite among major carbonate producers is opposite to what is expected due to the increase of seawater Mg/Ca in the Late Cretaceous.

Proxies for Cretaceous environmental change are available at different time scales, that is with different temporal resolutions. Events of turnover and extinction among major carbonate producers may be the results of events that unfolded on time scales of 10s–100s kyrs. While

there is significant current progress in the identification, quantification, and correlation of such events in hemipelagic environments, more work is needed to achieve similar progress in the rather fragmentary archives of Cretaceous carbonate platforms, which are more difficult to correlate, but – by analogy to modern environments – were hotspots of marine biodiversity. High-resolution stratigraphic studies are required to better constrain the causal factor among the environmental perturbations that occurred in the context of OAEs, and which resulted in the rise and demise of major benthic carbonate producers.

Declaration of Competing Interest

The authors declare that they have no known competing financial interests or personal relationships that could have appeared to influence the work reported in this paper.

Data availability

data are included in supplementary materials

Acknowledgements

MP was partially funded by the MIUR under the grant PRIN2017 RX9XXXY. Valuable comments of two anonymous reviewers are gratefully acknowledged.

Appendix A. Supplementary data

Supplementary data to this article can be found online at https://doi.org/10.1016/j.earscirev.2023.104341.

References

Abramovich, S., Keller, G., Stüben, D., Berner, Z., 2003. Characterization of late Campanian and Maastrichtian planktonic foraminiferal depth habitats and vital activities based on stable isotopes. Palaeogeogr. Palaeoclimatol.Palaeoecol. 202, 1–29. https://doi.org/10.1016/S0031-0182(03)00572-8.

Adloff, M., Greene, S.E., Parkinson, I.J., Naafs, D.A., Preston, W., Ridgwell, A., Lunt, D.J., Castro Jiménez, J.M., Monteiroa, F.M., 2020. Unravelling the sources of carbon emissions at the onset of Oceanic Anoxic Event (OAE) 1a. Earth Planet. Sci. Lett. 530, 115947 https://doi.org/10.1016/j.epsl.2019.115947.

Aguirre, J., Riding, R., 2005. Dasycladalean algal biodiversity compared with global variations in temperature and sea level over the past 350 Myr. Palaios 20, 581–588. https://doi.org/10.2110/palo.2004.p04-33.

Allemand, D., Ferrier-Pagès, C., Furla, P., Houlbrèque, F., Tambutté, E., Tambutté, S., Zoccola, D., 2004. Biomineralization in reef-building corals: from molecular mechanisms to environmental control. C. R. Palevol. 3, 453–467. https://doi.org/10.1016/j.crpv.2004.07.011.

Alroy, J., Marshall, C.R., Bambach, R.K., Bezuskoe, K., Foote, M., Fürsich, F.T., Hansen, T.A., Holland, S.M., Ivany, L.C., Jablonski, D., Jacobs, D.K., Jones, D.C., Kosnik, M.A., Lidgard, S., Low, S., Miller, A.I., Novack-Gottshall, P.M., Olszewski, T. D., Patzkowsky, M.E., Raup, D.M., Roy, K., Sepkoski, J.J., Sommers, M.G., Wagner, P.J., Webber, A., 2001. Effects of sampling standardization on estimates of Phanerozoic marine diversification. Proc. Natl. Acad. Sci. 98, 6261–6266.

Amodio, S., Weissert, H., 2017. Palaeoenvironment and palaeoecology before and at the onset of Oceanic Anoxic Event (OAE)1a: reconstructions from Central Tethyan archives. Palaeogeogr., PalaeoclimatolPalaeoecol. 479, 71–89. https://doi.org/10.1016/j.palaeo.2017.04.018.

Balthasar, U., Cusack, M., 2015. Aragonite-calcite seas—quantifying the gray area. Geology 43, 99–102. https://doi.org/10.1130/G36293.1.

Bambach, R.K., Knoll, A.H., Sepkoski, J.J., 2002. Anatomical and ecological constraints on Phanerozoic animal diversity in the marine realm. Proc. Natl. Acad. Sci. 99, 6854–6859. https://doi.org/10.1073/pnas.092150999.

Barker, S., Elderfield, H., 2002. Foraminiferal calcification response to glacial – interglacial changes in atmospheric CO2. Science 297, 833–836. https://doi.org/10.1126/science.1072815.

Barnes, D.J., Chalker, B.E., 1990. Calcification and photosynthesis in reef-building corals and algae. In: Dubinsky, Z. (Ed.), Coral Reefs. Elsevier, Amsterdam, pp. 109–131.

Bauer, K.W., Zeebe, R.E., Wortmann, U.G., 2017. Quantifying the volcanic emissions which triggered Oceanic Anoxic Event 1a and their effect on ocean acidification. Sedimentology 64, 204–2014. https://doi.org/10.1111/sed.12335.

Beil, S., Kuhnt, W., Holbourn, A., Scholz, F., Oxmann, J., Wallmann, K., Lorenzen, J., Aquit, M., Chellai, E.H., 2020. Cretaceous oceanic anoxic events prolonged by phosphorus cycle feedbacks. Clim. Past 16, 757–782. https://doi.org/10.5194/cp-16-757-2020.

Berger, S., Kaever, M.J., 1992. Dasycladales: An Illustrated Monograph of a Fascinating Algal Order, 247 pp. Georg Thieme, Stuttgart.

Billard, C., Inouye, I., 2004. What is new in coccolithophore biology? In: Thierstein, H.R., Young, J.R. (Eds.), Coccolithophores–from Molecular Processes to Global Impact. Springer, Berlin, Heidelberg, pp. 1–30.

Bodin, S., Meissner, P., Janssen, N.M.M., Steuber, T., Muttelose, J., 2015. Large igneous provinces and organic carbon burial: controls on global temperature and continental weathering during the Early Cretaceous. Glob. Planet. Change 133, 238–253. https://doi.org/10.1016/j.gloplacha.2015.09.001.

Bornemann, A., Norris, R.D., 2007. Size-related stable isotope changes in Late Cretaceous planktic foraminifera: implications for paleoecology and photosymbiosis. Mar. Micropaleontol. 65, 32–42. https://doi.org/10.1016/j.marmicro.2007.05.005.

Borowitzka, M.A., 1986. Physiology and biochemistry of calcification in the Chlorophyceae. In: Leadbeater, B.S.C., Riding, R. (Eds.), Biomineralization in Lower Plants and Animals. Systematics Assoc., Spec, Vol. 30, pp. 107–124.

Bosscher, H., Schlager, W., 1993. Accumulation rates of carbonate platforms. J. Geol. 101, 345–355.

BouDagher-Fadel, M.K., 2018. Evolution and geological significance of Larger Benthic Foraminifera. In: UCL Press, p. 693 pp.. https://doi.org/10.2307/j.ctvqhsq3.

Bown, P.R., Lees, J.A., Young, J.R., 2004. Calcareous nannoplankton evolution and diversity through time. In: Thierstein, H.R., Young, J.R. (Eds.), Coccolithophores–from Molecular Processes to Global Impact. Springer, Berlin, Heidelberg, pp. 481–508. https://doi.org/10.1007/978-3-662-06278-4_18.

Bown, P., Huber, B., Wade, B., Young, J., 2022. Mikrotax website. <mikrotax.org/pforams&gt.

Broecker, W., Clark, E., 2009. Ratio of coccolith CaCO3 to foraminifera CaCO3 in late Holocene deep sea sediments. Paleoceanography 24. https://doi.org/10.1029/2009PA001731. PA3205.

Broecker, W., Yu, J., 2011. What do we know about the evolution of Mg to ca rations in seawater? Paleoceanography 26. https://doi.org/10.1029/2011PA002120. PA3203.

Byrne, M., Przeslawski, R., 2013. Multistressor impacts of warming and acidification of the ocean on marine invertebrates' life histories. Integr. Comp. Biol. 53, 582–596. https://doi.org/10.1093/icb/ict049.

Cairns, S.D., Kitahara, M.V., 2012. An illustrated key to the genera and subgenera of the recent azooxanthellate Scleractinia (Cnidaria, Anthozoa), with an attached glossary. Zookeys 227, 1–47. https://doi.org/10.3897/zookeys.227.3612.

Cameron, L.P., Reymond, C.E., Müller-Lundin, F., Westfield, I., Grabowski, J.H., Westphal, H., Ries, J., 2019. Effects of temperature and ocean acidification on the extrapallial fluid pH, calcification rate, and condition factor of the king scallop Pecten maximus. J. Shellfish Res. 38, 763–777. https://doi.org/10.2983/035.038.0327.

Cao, W., Zahirovic, S., Flament, N., Williams, S., Golonka, J., Müller, R.D., 2017. Improving global paleogeography since the late Paleozoic using paleobiology. Biogeosciences 14, 5425–5439. https://doi.org/10.5194/bg-14-5425-2017.

Castro, J.M., Ruiz-Ortiz, P.A., de Gea, G.A., Aguado, R., Jarvis, I., Weissert, H., Molina, J. M., Nieto, L.M., Pancost, R.D., Quijano, M.L., Reolid, M., Skelton, P.W., López-Rodríguez, C., Martínez-Rodríguez, R., 2021. High-resolution C-isotope, TOC and biostratigraphic records of OAE 1a (Aptian) from an expanded hemipelagic cored succession, western Tethys: a new stratigraphic reference for global correlation and paleoenvironmental reconstruction. Paleoceanogr. Paleoclimatol. 36, e2020PA004004 https://doi.org/10.1029/2020PA004004.

Cavalheiro, L., Wagner, T., Steunig, S., Bottini, C., Dummann, W., Esegbue, O., Gambacorta, G., Giraldo-Gómez, V., Farnsworth, A., Flögel, S., Hofmann, P., Lunt, D. J., Rethemeyer, J., Torricelli, S., Erba, E., 2021. Impact of global cooling on early cretaceous high pCO2 world during the Weissert Event. Nat. Commun. 12, 5411. https://doi.org/10.1038/s41467-021-25706-0.

Close, R., Benson, R.B.J., Saupe, E., Clapham, M., Butler, R., 2020. The spatial structure of marine animal diversity. Science 386, 420–424. https://doi.org/10.1126/science.aay8309.

Debenay, J.-P., Guillou, J.-J., Geslin, E., Lesourd, M., 2000. Crystallization of calcite in foraminiferal tests. Micropaleontology 46 (supplement 1), 87–94.

Demicco, R.V., Lowenstein, T.K., Hardie, L.A., Spencer, R.J., 2005. Model of seawater composition for the Phanerozoic. Geology 33, 877–880. https://doi.org/10.1130/G21945.1.

Nooijer, De, Toyofuku, T., Kitazato, H., 2009. Foraminifera promote calcification by elevating their intracellular pH. Proc. Natl. Acad. Sci. 106, 15374–15378. https://doi.org/10.1073/pnas.0904306106.

De Nooijer, L.D., Spero, H.J., Erez, J., Bijma, J., Reichart, G.J., 2014. Biomineralization in perforate foraminifera. Earth-Sci. Rev. 135, 48–58. https://doi.org/10.1016/j.earscirev.2014.03.013.

D'Hondt, S.D., Zachos, J.C., 1998. Cretaceous foraminifera and the evolutionary history of planktic photosymbiosis. Paleobiology 24, 512–523. https://doi.org/10.1017/S0094837300020133.

Dias, B.B., Hart, M.B., Smart, C.W., Hall-Spencer, J.M., 2010. Modern seawater acidification: the response of foraminifera to high-CO2 conditions in the Mediterranean Sea. J. Geol. SocLondon 167, 843–846. https://doi.org/10.1144/0016-76492010-050.

Dong, Shuaishuai, Lei, Yanli, Li, Tiegang, Jian, Zhimin, 2020. Response of benthic foraminifera to pH changes: community structure and morphological transformation studies from a microcosm experiment. Mar. Micropaleontol. 156, 101819 https://doi.org/10.1016/j.marmicro.2019.101819.

Doo, S.S., Fujita, K., Byrne, M., Uthicke, S., 2014. Fate of calcifying tropical symbiont-bearing large benthic foraminifera: living sands in a changing ocean. Biol. Bull. 226, 169–186. https://doi.org/10.1086/BBLv226n3p169.

Drzewiecki, P.A., Simo, J.T., 2000. Tectonic, eustatic and environmental controls on mid-cretaceous carbonate platform deposition, south-central Pyrenees, Spain. Sedimentology 47, 471–495. https://doi.org/10.1046/j.1365-3091.2000.00286.x.
Dubicka, Z., 2019. Chamber arrangement versus wall structure in the highrank phylogenetic classification of Foraminifera. Acta Palaeontol. Pol. 64, 1–18. https://doi.org/10.4202/app.00564.2018.
Dubicka, Z., Owocki, K., Gloc, M., 2018. Micro- and nanostructures of calcareous foraminiferal tests: insights from representatives of Miliolida, Rotaliida and Lagenida. J. Foraminifer. Res. 48, 142–155. https://doi.org/10.2113/gsjfr.48.2.142.
Dutkiewicz, A., Müller, R.D., Cannon, J., Vaughan, S., Zahirovic, S., 2019. Sequestration and subduction of deep-sea carbonate in the global ocean since the early cretaceous. Geology 47, 91–94. https://doi.org/10.1130/G45424.1.
Eichenseer, K., Balthasar, U., Smart, C.W., Stander, J., Haaga, K.A., Kiessling, W., 2019. Jurassic shift from abiotic to biotic control on marine ecological success. Nature Geosci. 12, 638–642. https://doi.org/10.1038/s41561-019-0392-9.
Elbrächter, M., Gottschling, M., Hildebrand-Habel, T., Keupp, H., Kohring, R., Lewis, J., Meier, K.J.S., Montresor, M., Streng, M., Versteegh, G.J.M., Willems, H., Zonneveld, K., 2008. Establishing an agenda for calcareous dinoflagellate research (Thoracosphaeraceae, Dinophyceae) including a nomenclatural synopsis of generic names. Taxon 57, 1289–1303. https://doi.org/10.1002/tax.574019.
Erba, E., 1994. Nannofossils and superplumes: the early Aptian "nannoconid crisis". Paleoceanography 9, 483–501. https://doi.org/10.1029/94PA00258.
Erba, E., 2004. Calcareous nannofossils and Mesozoic oceanic anoxic events. Mar. Micropaleontol. 52, 85–106. https://doi.org/10.1016/j.marmicro.2004.04.007.
Erba, E., 2006. The first 150 million years history of calcareous nannoplankton: biosphere–geosphere interactions. Palaeogeogr. Palaeoclimatol.Palaeoecol. 232, 237–250. https://doi.org/10.1016/j.palaeo.2005.09.013.
Erba, E., Bottini, C., Weissert, H.J., Keller, C.E., 2010. Calcareous nannoplankton response to surface-water acidification around oceanic anoxic event 1a. Science 329, 428–432. https://doi.org/10.1126/science.1188886.
Erez, J., 2003. The source of ions for biomineralization in foraminifera and their implications for paleoceanographic proxies. In: Dove, P.M., Yoreo, J.J.D., Weiner, S. (Eds.), Biomineralization. Rev. Mineral. Geochem. 54, pp. 115–149. https://doi.org/10.1515/9781501509346-010.
Falkowski, P.G., Katz, M.E., Knoll, A.H., Quigg, A., Raven, J.A., Schofield, O., Taylor, F.J. R., 2004. The evolution of modern eukaryotic phytoplankton. Science 305, 354–360. https://doi.org/10.1126/science.1095964.
Fantle, M.S., Ridgwell, A., 2020. Towards an understanding of the ca isotopic signal related to ocean acidification and alkalinity overshoots in the rock record. Chem. Geol. 547, 119627 https://doi.org/10.1016/j.chemgeo.2020.119672.
Farinacci, A., Howe, R.W., 1969–2022.. The Farinacci & Howe Catalog of Calcareous Nannofossils, Vols 1–26. Accessed online at: mikrotax.org/Nannotax3/index.php?id=50002.
Fine, M., Tchernov, D., 2007. Scleractinian coral species survive and recover from decalcification. Science 315, 1811.
Finnegan, S., Anderson, S.C., Harnik, P.G., Simpson, C., Tittensor, D.P., Byrnes, J.E., Finkel, Z.V., Lindberg, D.R., Liow, L.H., Lockwood, R., Lotze, H.K., McClain, C.R., McGuire, J.L., O'Dea, A.J., Pandolfi, M., 2015. Paleontological baselines for evaluating extinction risk in the modern oceans. Science 348, 567–570. https://doi.org/10.1126/science.aaa6635.
Föllmi, K.B., 1995. 160 m.Y. Record of marine sedimentary phosphorus burial: Coupling of climate and continental weathering under greenhouse and icehouse conditions. Geology 23, 503–506. https://doi.org/10.1130/0091-7613(1995)023<0503:MYROMS>2.3.CO;2.
Föllmi, K.B., 2012. Early cretaceous life, climate and anoxia. Cretac. Res. 35, 230–257. https://doi.org/10.1016/j.cretres.2011.12.005.
Föllmi, K.B., Godet, A., 2013. Palaeoceanography of Lower Cretaceous Alpine platform carbonates. Sedimentology 60, 131–151. https://doi.org/10.1111/sed.12004.
Foote, M.J., Crampton, J.S., Beu, A.G., Nelson, C.S., 2015. Aragonite bias, and lack of bias, in the fossil record: lithological, environmental, and ecological controls. Paleobiology 41, 245–265. https://doi.org/10.1017/pab.2014.16.
Forster, A., Schouten, S., Baas, M., Sinninghe Damsté, J.S., 2007. Mid-Cretaceous (Albian-Santonian) sea surface temperature record of the tropical Atlantic Ocean. Geology 35, 919–922. https://doi.org/10.1130/G23874A.1.
Foster, G.L., Royer, D., Lunt, D.J., 2017. Future climate forcing potentially without precedent in the last 420 million years. Nat. Commun. 6, 14845. https://doi.org/10.1038/ncomms14845.
Foster, G., Hull, P., Lunt, D.J., Zachos, J., 2018. Placing our current 'hyperthermal' in the context of rapid climate change in our geological past. Phil. Trans. R. Soc. A 376, 20170086. https://doi.org/10.1098/rsta.2017.0086.
Friedrich, O., Norris, R.D., Erbacher, J., 2012. Evolution of middle to Late Cretaceous oceans - a 55 m.y. record of Earth's temperature and carbon cycle. Geology 40, 107–110. https://doi.org/10.1130/G32701.1.
Gibbs, S.J., Robinson, S.A., Bown, P.R., Jones, T.D., Henderiks, J., 2011. Comment on "Calcareous Nannoplankton Response to Surface-Water Acidification around Oceanic Anoxic Event 1a". Science 332, 175-b. https://doi.org/10.1126/science.1199459.
Gili, E., Götz, S., 2018. In: Paleoecology of rudists. Part N, Volume 2, Chapter 26B: Paleoecology of rudists. Treatise Online 103, pp. 1–29. https://doi.org/10.17161/to.v0i0.7183.
Gili, E., Masse, J.-P., Skelton, P.W., 1995. Rudists as gregarious sediment-dwellers, not reef-builders, on Cretaceous carbonate platforms. Palaeogeogr. Palaeoclimatol. Palaeoecol. 118, 245–267. https://doi.org/10.1016/0031-0182(95)00006-X.
Gradstein, F.M., Ogg, J.G., Schmitz, M., Ogg, G., 2012. The Geologic Time Scale 2012. Elsevier, 1144 p.
Granier, B., 2012. The contribution of calcareous green algae to the production of limestones: a review. Geodiversitas 34, 35–60. https://doi.org/10.5252/g2012n1a3.
Granier, B., Deloffre, R., 1993. Inventaire des algues dasycladales fossiles. II° partie - Les algues dasycladales du Jurassique et du Crétacé. Rev. Paléobiol. 12, 19–65.
Hain, M.P., Sigman, D.M., Higgins, J.A., Haug, G.H., 2015. The effects of secular calcium and magnesium concentration changes on the thermodynamics of seawater acid/base chemistry: implications for Eocene and Cretaceous ocean carbon chemistry and buffering. Glob. Biogeochem. Cycles 29, 517–533. https://doi.org/10.1002/2014GB004986.
Hallock, P., 1981. Production of carbonate sediments by selected large benthic foraminifera on two Pacific coral reefs. J. Sediment. Petrol. 51, 467–474. https://doi.org/10.1306/212F7CB1-2B24-11D7-8648000102C1865D.
Hallock, P., 1985. Why are larger foraminifera large? Paleobiology 11, 457–471. https://doi.org/10.1017/S0094837300011507.
Hallock, P., 1987. Fluctuations in the trophic resource continuum: a factor in global diversity cycles? Paleoceanogr. Paleoclimatol. 2, 457–471. https://doi.org/10.1029/PA002i005p00457.
Hallock, P., 2001. Coral reefs, carbonate sediments, nutrients, and global change. In: Stanley, G.D. (Ed.), The History and Sedimentology of Ancient Reef Systems. Top. Geobiol. 17. Springer, Boston, MA, pp. 387–427. https://doi.org/10.1007/978-1-4615-1219-6_11.
Hallock, P., Schlager, W., 1986. Nutrient excess and the demise of coral reefs and carbonate platforms. Palaios 1, 389–398.
Hannisdal, B., Peters, S.E., 2011. Phanerozoic Earth system evolution and marine biodiversity. Science 334, 1121–1124. https://doi.org/10.1126/science.1210695.
Harnik, P.G., Lotze, H.K., Anderson, S.C., Finkel, Z.V., 2012. Extinctions in ancient and modern seas. Trends Ecol. Evol. 27, 608–617. https://doi.org/10.1016/j.tree.2012.07.010.
Harvey, B.P., Gwynn-Jones, D., Moore, P.J., 2013. Meta-analysis reveals complex marine biological responses to the interactive effects of ocean acidification and warming. Ecol. Evol. 3, 1016–1030. https://doi.org/10.1002/ece3.516.
Hautmann, M., 2004. Effect of end-Triassic CO2 maximum on carbonate sedimentation and marine mass extinction. Facies 50, 257–261. https://doi.org/10.1007/s10347-004-0020-y.
Hay, W.W., 2004. Carbonate fluxes and calcareous nannoplankton. In: Thierstein, H.R., Young, J.R. (Eds.), Coccolithophores–from Molecular Processes to Global Impact. Springer, Berlin, Heidelberg, pp. 509–528. https://doi.org/10.1007/978-3-662-06278-4_19.
Hay, W.W., 2009. Cretaceous oceans and ocean modeling. In: Hu, Xiumian, Wang, Chengshan, Scott, R.W., Wagreich, M., Jansa, L. (Eds.), Cretaceous Oceanic Red Beds: Stratigraphy, Composition, Origins, and Paleoceanographic and Paleoclimatic Significance. SEPM Spec. Publ. 91, pp. 243–271. https://doi.org/10.2110/sepmsp.091.243.
Heiss, G.A., 1995. Carbonate production by scleractinian corals at Aqaba, Gulf of Aqaba, Red Sea. Facies 33, 19–34.
Hermoso, M., 2015. Control of ambient pH on growth and stable isotopes in phytoplanktonic calcifying algae. Paleoceanography 30, 1100–1112. https://doi.org/10.1002/2015PA002844.
Hönisch, B., Ridgwell, A., Schmidt, D.N., Thomas, E., Gibbs, S.J., Sluijs, A., Zeebe, R., Kump, L., Martindale, R.C., Greene, S.E., Kiessling, W., Ries, J., Zachos, J.C., Royer, D.L., Barker, S., Marchitto Jr., T.M., Moyer, R., Pelejero, C., Ziveri, P., Foster, G.L., Williams, B., 2012. The geological record of ocean acidification. Science 335, 1058–1063. https://doi.org/10.1126/science.1208277.
Hottinger, L., 1982. Larger foraminifera, giant cells with a historical background. Naturwissenschaften 69, 361–371.
Houston, R.M., Huber, B.T., 1998. Evidence of photosymbiosis in fossil taxa? Ontogenetic stable isotope trends in some Late Cretaceous planktonic foraminifera. Mar. Micropaleontol. 34, 29–46. https://doi.org/10.1016/S0377-8398(97)00038-8.
Huber, B.T., Leckie, R.M., 2011. Planktonic foraminiferal species turnover across deep-sea Aptian/Albian boundary sections. J. Foraminifer. Res. 41, 53–95. https://doi.org/10.2113/gsjfr.41.1.53.
Huber, B.T., MacLeod, K.G., Watkins, D.K., Coffin, M.F., 2018. The rise and fall of the Cretaceous hot greenhouse climate. Glob. Planet. Change 187, 1–23. https://doi.org/10.1016/j.gloplacha.2018.04.004.
Huck, S., Rameil, N., Korbar, T., Heimhofer, U., Wieczorek, D.T., Immenhauser, A., 2010. Latitudinally different responses of Tethyan shoal-water carbonate systems to the Early Aptian oceanic anoxic event (OAE 1a). Sedimentology 57, 1585–1614. https://doi.org/10.1111/j.1365-3091.2010.01157.
Huck, S., Heimhofer, U., Immenhauser, A., 2012. Early Aptian algal bloom in a neritic proto–North Atlantic setting: harbinger of global change related to OAE 1a? GSA Bull. 123, 1810–1825. https://doi.org/10.1130/B30587.1.
Hume, B.C.C., Voolstra, C.R., Arif, C., D'Angelo, C., Burt, J.A., Eyal, G., Loya, Y., Wiedenmann, J., 2016. Ancestral genetic diversity associated with the rapid spread of stress-tolerant coral symbionts in response to Holocene climate change. Proc. Natl. Acad. Sci. 113, 4416–4421. https://doi.org/10.1073/pnas.1601910113.
Jackson, J.B.C., Johnson, K.G., 2001. Measuring past biodiversity. Science 293, 2401–2404. https://doi.org/10.1126/science.1063789.
Jacob, D.E., Wirth, R., Agbaje, O.B.A., Branson, O., Eggins, S.M., 2017. Planktic foraminifera form their shells via metastable carbonate phases. Nat. Commun. 8, 1265. https://doi.org/10.1038/s41467-017-00955-0.
Jarvis, I., Mabrouk, A., Moody, R.T.J., de Cabrera, S., 2002. Late Cretaceous (Campanian) carbon isotope events, sea-level change and correlation of the Tethyan and Boreal realms. Palaeogeogr., PalaeoclimatolPalaeoecol. 188, 215–248. https://doi.org/10.1016/S0031-0182(02)00578-3.
Jenkyns, H.C., 2010. Geochemistry of oceanic anoxic events. Geochem. Geophys. Geosyst. 11, Q03004. https://doi.org/10.1029/2009GC002788.

Jenkyns, H.C., 2018. Transient cooling episodes during Cretaceous Oceanic Anoxic events with special reference to OAE 1a (Early Aptian). Phil. Trans. R. Soc. A 376, 20170073. https://doi.org/10.1098/rsta.2017.0073.
Jenkyns, H.C., Wilson, P.A., 1999. Stratigraphy, paleoceanography, and evolution of cretaceous Pacific guyots; relics from a greenhouse Earth. Am. J. Sci. 299, 341–392. https://doi.org/10.2475/ajs.299.5.341.
Kawahata, H., Fujita, K., Iguchi, A., Inoue, M., Iwasaki, S., Kuroyanagi, A., Maeda, A., Manaka, T., Moriya, K., Takagi, H., Toyofuku, T., Yoshimura, T., Suzuki, A., 2019. Perspective on the response of marine calcifiers on global warming and ocean acidification – behavior of corals and foraminifera in a high CO2 world "hot house". Progr. Earth Planet. Sci. 6, 5. https://doi.org/10.1186/s40645-018-0239-9.
Kemp, D.B., Eichenseer, K., Kiessling, W., 2015. Maximum rates of climate change are systematically underestimated in the geological record. Nat. Commun. 6, 8890. https://doi.org/10.1038/ncomms9890.
Kenigsberg, C., Titelboim, D., Ashckenazi-Polivod, A.S., Herut, B., Kucera, M., Zukerman, Y., Hyams-Kaphzan, O., Almogi-Labin, A., Abramovich, S., 2022. The combined effects of rising temperature and salinity may halt the future proliferation of symbiont-bearing foraminifera as ecosystem engineers. Sci. Total Environ. 806, 150581 https://doi.org/10.1016/j.scitotenv.2021.150581.
Kiessling, W., Flügel, E., Golonka, J., 2000. Fluctuations in the carbonate production of Phanerozoic reefs. In: Insalaco, E., Skelton, P.W., Palmer, T.J. (Eds.), Carbonate Platform Systems: Components and Interactions. Geol. Soc., London, Spec. Publ. 178, pp. 191–215. https://doi.org/10.1144/GSL.SP.2000.178.01.13.
Kiessling, W., Flügel, E., Golonka, J., 2003. Patterns of Phanerozoic carbonate platform sedimentation. Lethaia 36, 195–225. https://doi.org/10.1080/00241160310004648.
Kiessling, W., Aberhan, M., Villier, L., 2008. Phanerozoic trends in skeletal mineralogy driven by mass extinctions. Nat. Geosci. 1, 527–530.
Kiessling, W., Kocsis, A., 2015. Biodiversity dynamics and environmental occupancy of fossil azooxanthellate and zooxanthellate scleractinian corals. Paleobiology 41, 402–414. https://doi.org/10.1017/pab.2015.6.
Korbar, T., Glumac, B., Tešović, B.C., Cadieux, S.B., 2012. Response of a carbonate platform to the Cenomanian-Turonian drowning and OAE 2: a case study from the Adriatic platform (Dalmatia, Croatia). J. Sediment. Res. 82, 163–176. https://doi.org/10.2110/jsr.2012/17.
Kuhnt, W., Holbourn, A.E., Beil, S., Aquit, M., Krawczyk, T., Flögel, S., Chellai, E.H., Jabour, H., 2017. Unraveling the onset of cretaceous Oceanic Anoxic Event 2 in an extended sediment archive from the Tarfaya- Laayoune Basin, Morocco. Paleoceanography 32, 923–946. https://doi.org/10.1002/2017PA003146.
Kuroyanagi, A., Kawahata, H., Ozaki, K., Suzuki, A., Nishi, H., Takashima, R., 2020. What drove the evolutionary trend of planktic foraminifers during the cretaceous: Oceanic Anoxic events (OAEs) directly affected it? Mar. Micropaleontol. 161, 101924 https://doi.org/10.1016/j.marmicro.2020.101924.
Langer, M., 2008. Assessing the contribution of foraminiferan protists to Global Ocean carbonate production. J. Eukaryot. Microbiol. 55, 163–169. https://doi.org/10.1111/j.1550-7408.2008.00321.x.
Lechler, M., Pogge von Strandmann, P.A.E., Jenkyns, H.C., Prosser, G., Parente, M., 2015. Lithium-isotope evidence for enhanced silicate weathering during OAE1a (Early Aptian Selli event). Earth Planet. Sci. Lett. 432, 210–222. https://doi.org/10.1016/j.epsl.2015.09.052.
Leckie, R.M., Bralower, T.J., Cashman, R., 2002. Oceanic anoxic events and plankton evolution: biotic response to tectonic forcing during the mid-Cretaceous. Paleoceanography 17. https://doi.org/10.1029/2001PA000623, 13.1–13.29.
Lee, J.J., 2006. Algal symbiosis in larger foraminifera. Symbiosis 42, 63–75.
Lee, J.J., Hallock, P., 1987. Algal symbiosis as the driving force in the evolution of larger foraminifera. Ann. N. Y. Acad. Sci. 503, 330–347. https://doi.org/10.1111/j.1749-6632.1987.tb40619.x.
Leung, J.Y.S., Zhang, S., Connell, S.D., 2022. Is ocean acidification really a threat to marine calcifiers? A systematic review and meta-analysis of 980+ studies spanning two decades. Small 18, 2107407. https://doi.org/10.1002/smll.202107407.
Linnert, C., Mutterlose, J., Erbacher, J., 2010. Calcareous nannofossils of the Cenomanian/Turonian boundary interval from the Boreal Realm (Wunstorf, Northwest Germany). Mar. Micropaleontol. 74, 38–58. https://doi.org/10.1016/j.marmicro.2009.12.002.
Loeblich Jr., A.R., Tappan Jr., H., 1988. Foraminiferal Genera and their Classification, 2 vol.. Van Nostrand Reinhold, New York, 2047pp.
Lombard, F., Labeyrie, L., Michel, E., Bopp, L., Cortijo, E., Retailleau, S., Howa, H., Jorissen, F., 2011. Modelling planktic foraminifer growth and distribution using an ecophysiological multi-species approach. Biogeosciences 8, 853–873. https://doi.org/10.5194/bg-8-853-2011.
Löser, H., 2016. In: Systematic Part. – Catalogue of Cretaceous Corals, vol. 4. Dresden (CPress Verlag), pp. 1–710.
Lowenstein, T.K., Timofeeff, M.N., Brennan, S.T., Hardie, L.A., Demicco, R.V., 2001. Oscillations in Phanerozoic seawater chemistry: evidence from fluid inclusions. Science 294, 1086–1088. https://doi.org/10.1126/science.1064280.
Lowery, C.M., Bown, P.R., Fraas, A.J., Hull, P.M., 2020. Ecological response of plankton to environmental change: thresholds for extinction. Annu. Rev. Earth Planet. Sci. 48 https://doi.org/10.1146/annurev-earth-081619-052818, 16.1–16.27.
Matsumoto, H., Coccioni, R., Frontalini, F., Shirai, K., Jovane, L., Trindade, R., Savian, J. F., Kuroda, J., 2022. Mid-Cretaceous marine Os isotope evidence for heterogeneous cause of oceanic anoxic events. Nat. Commun. 13, 239. https://doi.org/10.1038/s41467-021-27817-0.
Mattioli, E., Pittet, B., Riquier, L., Grossi, V., 2014. The mid-Valanginian Weissert Event as recorded by calcareous nannoplankton in the Vocontian Basin. Palaeogeogr. PalaeoclimatolPalaeoecol. 414, 472–485. https://doi.org/10.1016/j.palaeo.2014.09.030.
Miller, K.G., Kominz, M.A., Browning, J.V., Wright, J.D., Mountain, G.S., Katz, M.E., Sugarman, P.J., Cramer, B.S., Christie-Blick, N., Pekar, S.F., 2005. The Phanerozoic record of sea-level change. Science 310, 1293–1298. https://doi.org/10.1126/science.1116412.
Molina, E., 2015. Evidence and causes of the main extinction events in the Paleogene based on extinction and survival patterns of foraminifera. Earth-Sci. Rev. 140, 166–181. https://doi.org/10.1016/j.earscirev.2014.11.008.
Morse, J.W., Wang, Q., Tsio, M.Y., 1997. Influences of temperature and Mg: ca ratio on CaCO3 precipitates from seawater. Geology 25, 85–87. https://doi.org/10.1130/0091-7613(1997)025<0085:IOTAMC>2.3.CO;2.
Mutterlose, J., Bottini, C., 2013. Early Cretaceous chalks from the North Sea giving evidence for global change. Nat. Commun. 4, 1686. https://doi.org/10.1038/ncomms2698.
Mutti, M., Hallock, P., 2003. Carbonate systems along nutrient and temperature gradients: some sedimentological and geochemical constraints. Intern. J. Earth Sci. 92, 465–475. https://doi.org/10.1007/s00531-003-0350-y.
Navarro-Ramirez, J.P., Bodin, S., Consorti, L., Immenhauser, A., 2017. Response of western South american epeiric-neritic ecosystem to middle cretaceous Oceanic Anoxic events. Cretac. Res. 75, 61–80. https://doi.org/10.1016/j.cretres.2017.03.009.
Narayan, G.R., Reymond, C.E., Stuhr, M., Doo, S., Schmidt, C., Mann, T., Westphal, H., 2022. Response of large benthic foraminifera to climate and local changes: ḷmplications for future carbonate production. Sedimentology 69, 121–161. https://doi.org/10.1111/sed.12858.
Newell, N.D., 1965. Classification of the Bivalvia. Am. Mus. Novitates 2206, 25 pp.
O'Brien, C.L., Robinson, S.A., Pancost, R.D., Sinninghe Damsté, J.S., Schouten, S., Lunt, D.J., Alsenz, H., Bornemann, A., Bottini, C., Brassell, S.C., Farnsworth, A., Forster, A., Huber, B.T., Inglis, G.N., Jenkyns, H.C., Linnert, C., Littler, K., Markwick, P., McAnena, A., Mutterlose, J., Naafs, D.A., Püttmann, W., Sluijs, A., van Helmond, N., Vellekoop, J., Wagner, T., Wrobel, N.E., 2017. Cretaceous sea-surface temperature evolution: constraints from TEX86 and planktonic foraminiferal oxygen isotopes. Earth-Sci. Rev. 172, 224–247. https://doi.org/10.1016/j.earscirev.2017.07.012.
Odin, G.S., 2011. Gilianelles: Late Cretaceous microproblematica from Europe and Central America. Palaeontology 54, 133–144. https://doi.org/10.1111/j.1475-4983.2010.01012.x.
Opdyke, B.N., Wilkinson, B.H., 1990. Paleolatitude distribution of Phanerozoic marine ooids and cements. Palaeogeogr. PalaeoclimatolPalaeoecol. 78, 135–148. https://doi.org/10.1016/0031-0182(90)90208-O.
Oron, S., Evans, D., Abramovich, S., Almogi-Labin, A., Erez, J., 2020. Differential sensitivity of a symbiont-bearing foraminifer to seawater carbonate chemistry in a decoupled DIC-pH experiment. <sb:contribution><sb:title>J. Geophys. Res. </sb:title></sb:contribution><sb:host><sb:issue><sb:series><sb:title>Biogeosci.</sb:title></sb:series></sb:issue></sb:host> 125, e2020JG005726. https://doi.org/10.1029/2020JG005726.
Parente, M., Frijia, G., Di Lucia, M., Jenkyns, H.C., Woodfine, R.G., Baroncini, F., 2008. Stepwise extinction of larger foraminifers at the Cenomanian-Turonian boundary: a shallow-water perspective on nutrient fluctuations during Oceanic Anoxic Event 2 (Bonarelli Event). Geology 36, 715–718. https://doi.org/10.1130/G24893A.1.
Parker, J.H., 2017. Ultrastructure of the test wall in modern porcelaneous foraminifera: implicationsfor the classification of the Miliolida. J. Foraminif. Res. 47, 136–174. https://doi.org/10.2113/gsjfr.47.2.136.
Pascher, A., 1931. Systematische Übersicht über die mit Flagellaten in Zusammenhang stehenden Algenreihen und Versuch einer Einreihung dieser Algenstämme in die Stämme des Pflanzenreiches. Beih. Botan. Centralblatt 48 (Abteilung II, 2), 317–332.
Paul, C.R.C., Mitchell, S.F., 1994. Is famine a common factor in marine mass extinctions? Geology 22, 679–682. https://doi.org/10.1130/0091-7613(1994)022<0679:IFACFI>2.3.CO;2.
Pawlowski, J., Holzmann, M., Tyszka, J., 2013. New supraordinal classification of Foraminifera: molecules meet morphology. Mar. Micropaleontol. 100, 1–10. https://doi.org/10.1016/j.marmicro.2013.04.002.
Paytan, A., McLaughlin, K., 2007. The oceanic phosphorus cycle. Chem. Rev. 107, 563–576. https://doi.org/10.1021/cr0503613.
Penman, D.E., Kirtland Turner, S., Sexton, P.F., Norris, R.D., Dickson, A.J., Boulila, S., Ridgwell, A., Zeebe, R.E., Zachos, J.C., Cameron, A., Westerhold, T., Röhl, U., 2016. An abyssal carbonate compensation depth overshoot in the aftermath of the Palaeocene-Eocene thermal Maximum. Nat. Geosci. 9, 575–580. https://doi.org/10.1038/ngeo2757.
Perch-Nielsen, K., 1985. Mesozoic calcareous nannofossils. In: Bolli, H.M., Saunders, J.B., Perch-Nielsen, K. (Eds.), Plankton Stratigraphy, vol. 1. Cambridge University Press, Cambridge, UK, pp. 329–426.
Peters, S.E., Foote, M., 2001. Biodiversity in the Phanerozoic: a reinterpretation. Paleobiology 27, 583–601.
Peters, S.E., Kelly, D.C., Fraass, A.J., 2013. Oceanographic controls on the diversity and extinction of planktonic Foraminifera. Nature 493, 398–401. https://doi.org/10.1038/nature11815.
Philip, J., Airaud-Crumiere, C., 1991. The demise of the rudist-bearing carbonate platforms at the Cenomanian/Turonian boundary: a global control. Coral Reefs 10, 115–125. https://doi.org/10.1007/BF00571829.
Philip, J., Borgomano, J., Al-Maskiry, S., 1995. Cenomanian-Early Turonian carbonate platform of Northern Oman: stratigraphy and palaeo-environments. Palaeogeogr., PalaeoclimatolPalaeoecol. 119, 77–92. https://doi.org/10.1016/0031-0182(95)00061-5.
Pochon, X., Montoya-Burgos, J.I., Stadelmann, B., Pawlowski, J., 2006. Molecular phylogeny, evolutionary rates, and divergence timing of the symbiotic dinoflagellate

genus Symbiodinium. Mol. Phylogenet. Evol. 38, 20–30. https://doi.org/10.1016/j.ympev.2005.04.028.
Pohl, A., Laugié, M., Borgomano, J., Michel, J., Lanteaume, C., Scotese, C.R., Frau, C., Poli, E., Donnadieu, Y., 2019. Quantifying the paleogeographic driver of Cretaceous carbonate platform development using paleoecological niche modeling. Palaeogeogr., PalaeoclimatolPalaeoecol. 514, 222–232. https://doi.org/10.1016/j.palaeo.2018.10.017.
Pohl, A., Donnadieu, Y., Godderis, Y., Lanteaume, C., Hairabian, A., Frau, C., Michel, J., Laugie, M., Reijmer, J.J.G., Scotese, C.R., Borgomano, J., 2020. Carbonate platform production during the Cretaceous. GSA Bull. 132, 2606–2610. https://doi.org/10.1130/B35680.1.
Pomar, L., Hallock, P., 2008. Carbonate factories: a conundrum in sedimentary geology. Earth-Sci. Rev. 87, 134–169. https://doi.org/10.1016/j.earscirev.2007.12.002.
Price, G.D., Janssen, N.M.M., Martinez, M., Company, M., Vandevelde, J.H., Grimes, S.T., 2018. A high-resolution belemnite geochemical analysis of Early Cretaceous (Valanginian-Hauterivian) environmental and climatic perturbations. Geochem. GeophysGeosyst. 19, 3832–3843. https://doi.org/10.1029/2018GC007676.
Püttmann, T., Mutterlose, J., 2021. Paleoecology of Late Cretaceous coccolithophores: insights from the shallow-marine record. Paleoceanogr. Paleoclimatol. 36, e2020PA004161 https://doi.org/10.1029/2020PA004161.
Railsback, L.B., Anderson, T.F., 1987. Control of Triassic seawater chemistry and temperature on the evolution of post-Palaeozoic aragonite-secreting faunas. Geology 15, 1002–1005. https://doi.org/10.1130/0091-7613(1987)15<1002:COTSCA>2.0.CO;2.
Raja, R., Saraswati, P.K., Rogers, K., Iwao, K., 2005. Magnesium and strontium compositions of recent symbiont-bearing benthic foraminifera. Mar. Micropaleont. 58, 31–44. https://doi.org/10.1016/j.marmicro.2005.08.001.
Rameil, N., Immenhauser, A., Warrlich, G., Hillgärtner, H., Droste, H.J., 2010. Morphological patterns of Aptian Lithocodium-Bacinella geobodies: relation to environment and scale. Sedimentology 57, 883–911. https://doi.org/10.1111/j.1365-3091.2009.01124.
Raup, D.M., 1975. Taxonomic diversity estimation using rarefaction. Paleobiolog 1, 333–342.
Raup, D.M., 1976. Species diversity in the Phanerozoic: an interpretation. Paleobiology 2, 289–297.
Reddin, C.J., Kocsis, A.T., Aberhan, M., Kiessling, W., 2021. Victims of ancient hyperthermal events herald the fates of marine clades and traits under global warming. Glob. Change Biol. 27, 868–878. https://doi.org/10.1111/gcb.15434.
Ridgwell, A., 2005. A mid Mesozoic revolution in the regulation of ocean chemistry. Mar. Geol. 217, 339–357.
Riebesell, U., Zondervan, I., Rost, B., Tortell, P.D., Zeebe, R.E., Morel, F.M.M., 2000. Reduced calcification of marine plankton in response to increased atmospheric CO2. Nature 407, 364–367. https://doi.org/10.1038/35030078.
Ries, J.B., Cohen, A.L., McCorkle, D.C., 2009. Marine calcifiers exhibit mixed responses to CO2-induced ocean acidification. Geology 27, 1131–1134. https://doi.org/10.1130/G30210A.1.
Rigaud, S., Granier, B., Masse, J.P., 2021. Aragonitic foraminifers: an unsuspected wall diversity. J. System. Palaeontol. 19, 461–488. https://doi.org/10.1080/14772019.2021.1921863.
Ross, C.A., 1974. In: Evolutionary and ecological significance of large, calcareous Foraminiferida (Protozoa), Great Barrier Reef. Proc. 2nd IntCoral Reef Symp, 1, pp. 327–333.
Sadekov, A.Y., Bush, F., Kerr, J., Ganeshram, R., Elderfield, H., 2014. Mg/Ca composition of benthic foraminifera Miliolacea as a new tool of paleoceanography. Paleoceanography 29, 990–1001. https://doi.org/10.1002/2014PA002654.
Sandberg, P.A., 1983. An oscillating trend in Phanerozoic non-skeletal carbonate mineralogy. Nature 305, 19–22. https://doi.org/10.1038/305019a0.
Schiebel, R., 2002. Planktic foraminiferal sedimentation and the marine calcite budget. Glob. Biogeochem. Cycles 16. https://doi.org/10.1029/2001GB001459, 3–1–3-21.
Schiebel, R., Hemleben, C., 2017. Planktic Foraminifers in the Modern Ocean. In: Springer, p. 358 pp..
Schlanger, S.O., Jenkyns, H.C., 1976. Cretaceous oceanic anoxic events: causes and consequences. Geol. Mijnb. 55, 179–184.
Schlesinger, W.H., Bernhardt, E., 2020. Biogeochemistry - An Analysis of Climate Change. In: Elsevier, p. 749 pp..
Schmidt, D.N., Renaud, S., Bollmann, J., Schiebel, R., Thierstein, H.R., 2004. Size distribution of Holocene planktic foraminifer assemblages: biogeography, ecology and adaptation. Mar. Micropaleontol. 50, 319–338. https://doi.org/10.1016/S0377-8398(03)00098-7.
Schmidt, C., Kucera, M., Uthicke, S., 2014. Combined effects of warming and ocean acidification on coral reef foraminifera Marginopora vertebralis and Heterostegina depressa. Coral Reefs 33, 805–818. https://doi.org/10.1007/s00338-014-1151-4.
Schmitt, K., Heimhofer, U., Frijia, G., di Lucia, M., Huck, S., 2020. Deciphering the fragmentary nature of cretaceous shallow-water limestone archives: a case study from the subtropical Apennine carbonate platform. Newsl. Stratigr. 53, 389–413. https://doi.org/10.1127/nos/2019/0551.
Les grands foraminifères du Crétacé moyen de la région méditerraniénne. In: Schroeder, R., Neumann, M. (Eds.), Geobios, Mém. Spec. 7, 160 pp.
Scotese, C.R., Song, H., Mills, B.J.W., van der Meer, D.G., 2021. Phanerozoic paleotemperatures: the earth's changing climate during the last 540 million years. Earth-Sci. Rev. 215, 103503 https://doi.org/10.1016/j.earscirev.2021.103503.
Scott, R.W., Fernández-Mendiola, P.A., Gili, E., Simo, A., 1990. Persistence of coral-rudist reefs into the late cretaceous. Palaios 5, 98–110. https://doi.org/10.2307/3514807.
Sen Gupta, B.K., 2003. Modern Foraminifera. In: Kluwer Academic Publishers, New York, p. 371 pp..
Skelton, P.W., 2003. The operation of the major geological carbon sinks. In: Skelton, P.W., Spicer, R.A., Kelley, S.P., Gilmour, I. (Eds.), The Cretaceous World. Cambridge University Press, Cambridge, England, pp. 259–266.
Skelton, P.W., 2018. In: Introduction to the Hippuritida (rudists): Shell structure, anatomy, and evolution. Treatise on Invertebrate Paleontology Online, Part N, Volume 1, Chapter 26A: Treatise Online 104. University of Kansas, Lawrence, pp. 1–37.
Skelton, P.W., Smith, A.B., 2000. A preliminary phylogeny of rudist bivalves: sifting clades from grades. In: Harper, E.M., Taylor, J.D., Crame, J.A. (Eds.), The Evolutionary Biology of the Bivalvia. Geol. Soc., London, Spec. Publ. 177, pp. 97–127.
Skelton, P., Gili, E., 2012. Rudists and carbonate platforms in the Aptian: a case study on biotic interactions with ocean chemistry and climate. Sedimentology 59, 81–117. https://doi.org/10.1111/j.1365-3091.2011.01292.
Skelton, P.W., Gili, E., Rosen, B.R., Valldeperas, F.X., 1997. Corals and rudists in the late Cretaceous: a critique of the hypotheses of competitive displacement. Bol. R. Soc. Esp. Hist. Nat. (Sec. Geol.) 92, 225–239.
Slater, S.M., Bown, P., Twitchett, R.J., Danise, S., Vajda, V., 2022. Global record of "ghost" nannofossils reveals plankton resilience to high CO2 and warming. Science 376, 853–856. https://doi.org/10.1126/science.abm7330.
Smith, A.B., Gale, A.S., Monks, N.E.A., 2001. Sea-level change and rock-record bias in the cretaceous: a problem for extinction and biodiversity studies. Paleobiology 27, 241–253. https://doi.org/10.1666/0094-8373(2001)027<0241:SLCARR>2.0.CO;2.
Smith, B.P., Kerans, C., Fischer, W.W., 2021. A redox-based model for carbonate platform drowning and ocean anoxic events. Geophys. Res. Lett. 48, e2021GL093048 https://doi.org/10.1029/2021GL093048.
Spencer, C.J., 2022. Biogeodynamics: coupled evolution of the biosphere, atmosphere, and lithosphere. Geology 50, 867–868. https://doi.org/10.1130/GEOL50THAUG.1.
Stanley, S.M., 2008. Effects of global seawater chemistry on biomineralization: past, present, and future. Chem. Rev. 108, 4483–4498. https://doi.org/10.1021/cr800233u.
Stanley, S.M., Hardie, L.A., 1998. Secular oscillations in the carbonate mineralogy of reef-building and sediment-producing organisms driven by tectonically forced shifts in seawater chemistry. Palaeogeogr. PalaeoclimatolPalaeoecol. 144, 3–19.
Steuber, T., 1996. Stable isotope sclerochronology of rudist bivalves: growth rates and Late Cretaceous seasonality. Geology 24, 315–318. https://doi.org/10.1130/0091-7613(1996)024<0315:SISORB>2.3.CO;2.
Steuber, T., 2000. Skeletal growth rates of Upper Cretaceous rudist bivalves: implications for carbonate production and organism – environment feedbacks. In: Insalaco, E., Skelton, P.W., Palmer, T.J. (Eds.), Carbonate Platform Systems: Components and Interactions. Geol. Soc. Spec. Publ. 178, pp. 21–32. https://doi.org/10.1144/GSL.SP.2000.178.01.03.
Steuber, T., 2002. Plate tectonic control on the evolution of Cretaceous platform-carbonate production. Geology 30, 259–262. https://doi.org/10.1130/0091-7613(2002)030<0259:PTCOTE>2.0.CO;2.
Steuber, T., Löser, H., 2000. Species richness and abundance patterns of Tethyan Cretaceous rudist bivalves (Mollusca: Hippuritacea) in the Central-Eastern Mediterranean and Middle East, analysed from a palaeontological data base. Palaeogeogr., PalaeoclimatolPalaeoecol. 162, 75–104. https://doi.org/10.1016/S0031-0182(00)00106-1.
Steuber, T., Yilmaz, C., Löser, H., 1998. Growth rates of early Campanian rudists in a siliciclastic-calcareous setting (Pontid Mts., North-central Turkey). GeobiosMém. Spéc. 22, 385–401. https://doi.org/10.1016/S0016-6995(98)80088-0.
Steuber, T., Rauch, M., Masse, J.-P., Graaf, J., Malkoč, M., 2005. Low-latitude seasonality of Cretaceous temperatures in warm and cold episodes. Nature 437, 1341–1344. https://doi.org/10.1038/nature04096.
Steuber, T., Scott, R.W., Mitchell, S.F., Skelton, P.W., 2016. In: Stratigraphy and diversity dynamics of Jurassic-Cretaceous Hippuritida (rudist bivalves). Treatise on Invertebrate Paleontology Online, no. 81, Part N, Revised, Volume 1, Chapter 26C. University of Kansas, Lawrence, pp. 1–17.
Steuber, T., Alsuwaidi, M., Hennhoefer, D., Sulieman, H., AlBlooshi, A., McAlpin, T.D., Shebl, H., 2022. Environmental change and carbon-cycle dynamics during the onset of Cretaceous oceanic anoxic event 1a from a carbonate-ramp depositional system, Abu Dhabi, U.A.E. Palaeogeogr. Palaeoclimatol. Palaeoecol. 601, 111086 https://doi.org/10.1016/j.palaeo.2022.111086.
Stolarski, J., Meibom, A., Przenioslo, R., Mazur, M., 2007. A cretaceous scleractinian coral with a calcitic skeleton. Science 318, 92–94. https://doi.org/10.1126/science.1149237.
Stolarski, J., Bosellini, F.R., Wallace, C.C., Gothmann, A.M., Mazur, M., Domart-Coulon, I., Gutner-Hoch, E., Neuser, R.D., Levy, O., Shemesh, A., Meibom, A., 2016. A unique coral biomineralization pattern has resisted 40 million years of major ocean chemistry change. Sci. Rep. 6, 27579. https://doi.org/10.1038/srep27579.
Strohmenger, C.J., Steuber, T., Ghani, A., Barwick, D.G., Al-Mazrooei, S.H.A., Al-Zaabi, N.O., 2010. Sedimentology and chemostratigraphy of the Hawar and Shu'aiba depositional sequences, Abu Dhabi, United Arab Emirates. In: van Buchem, F.S.P., Al-Husseini, M.I., Maurer, F., Droste, H.J. (Eds.), Barremian – Aptian Stratigraphy and Hydrocarbon Habitat of the Eastern Arabian Plate. GeoArabia Spec. Publ. 4, pp. 341–365.
Suchéras-Marx, B., Mattioli, E., Allemand, P., Giraud, F., Pittet, B., Plancq, J., Escarguel, G., 2019. The colonization of the oceans by calcifying pelagic algae. Biogeosciences 16, 2501–2510. https://doi.org/10.5194/bg-16-2501-2019.
Sullivan, D.L., Brandon, A.D., Eldrett, J., Bergman, S.C., Wright, S., Minsini, D., 2020. High resolution osmium data record three distinct pulses of magmatic activity during cretaceous Oceanic Anoxic Event 2 (OAE-2). Geochim. Cosmochim. Acta 285, 257–273. https://doi.org/10.1016/j.gca.2020.04.002.

Surlyk, F., Dons, T., Clausen, C.K., Higham, J., 2003. Upper Cretaceous. In: Evans, D., Graham, C., Armour, A., Bathurst, P. (Eds.), The Millennium Atlas: Petroleum Geology of the Central and Northern North Sea. Geol. Soc, London, pp. 213–233.

Thierstein, H.R., 1979. Paleoceanographic implications of organic carbon and carbonate distribution in Mesozoic deepsea sediments. In: Talwart, M., Hy, W., Ryan, W.B.F. (Eds.), Deep Drilling Results in the Atlantic Ocean: Continental Margins and Paleoenvironments, vol. 3, pp. 249–274. https://doi.org/10.1029/ME003p0249.

Tomás, S., Löser, H., Salas, R., 2008. Low-light and nutrient-rich coral assemblages in an Upper Aptian carbonate platform of the southern Maestrat Basin (Iberian Chain, eastern Spain). Cretac. Res. 29, 509–534. https://doi.org/10.1016/j.cretres.2007.09.001.

Uličný, D., Hladíkov, J., Hradecká, L., 1993. Record of sea-level changes, oxygen depletion and the δ13C anomaly across the Cenomanian-Turonian boundary, Bohemian Cretaceous Basin. Cretac. Res. 14, 211–234. https://doi.org/10.1006/cres.1993.1015.

Uthicke, S., Momigliano, P., Fabricius, K.E., 2013. High risk of extinction of benthic foraminifera in this century due to ocean acidification. Sci. Rep. 3, 1769. https://doi.org/10.1038/srep01769.

van de Poel, H.M., Schlager, W., 1994. Variations in Mesozoic-Cenozoic skeletal carbonate mineralogy. Geol. Mijnb. 73, 31–51.

van Gorsel, J.T., 1978. Late Cretaceous orbitoidal foraminifera. In: Hedley, R.G., Adams, C.G. (Eds.), Foraminifera. Academic Press, London, pp. 1–120.

Vejbæk, O.V., Andersen, C., Dusar, M., Herngreen, G.F.W., Krabbe, H., Leszczyński, K., Lott, G.K., Mutterlose, J., Van der Molen, A.S., 2010. Cretaceous. In: Doornenbal, J. C., Stevenson, A.G. (Eds.), Petroleum Geological Atlas of the Southern Permian Basin Area. EAGE Publications b.v. (Houten), pp. 195–209.

Vilas, L., Masse, J.P., Arias, C., 1995. Orbitolina episodes in carbonate platform evolution: the early Aptian model from SE Spain. Palaeogeogr., PalaeoecolPalaeoclimatol. 119, 35–45. https://doi.org/10.1016/0031-0182(95)00058-5.

Voigt, S., 2000. Cenomanian-Turonian composite δ13C curve for Western and Central Europe: the role of organic and inorganic carbon fluxes. Palaeogeogr., PalaeoecolPalaeoclimatol. 160, 91–104. https://doi.org/10.1016/S0031-0182(00)00060-2.

Wang, Xin, Zoccola, D., Liew, Yi Jin, Tambutte, E., Cui, Guoxin, Allemand, D., Tambutte, S., Aranda, M., 2021. The evolution of calcification in reef-building corals. Mol. Biol. Evol. 38, 3543–3555. https://doi.org/10.1093/molbev/msab103.

Watson, A.J., Lenton, T.M., Mills, B.J.W., 2017. Ocean deoxygenation, the global phosphorus cycle and the possibility of human-caused large-scale ocean anoxia. Phil. Trans. R. Soc. A 375, 20160318. https://doi.org/10.1098/rsta.2016.0318.

Weissert, H., Erba, E., 2004. Volcanism, CO2 and palaeoclimate: a Late Jurassic-Early Cretaceous carbon and oxygen isotope record. J. Geol. Soc., LondonSpec. Publ. 161, 695–702. https://doi.org/10.1144/0016-764903-087.

Weissert, H., Lini, A., Föllmi, K.B., Kuhn, O., 1998. Correlation of Early Cretaceous carbon isotope stratigraphy and platform drowning events: a possible link? Palaeogeogr., Palaeoclimatol., Palaeoecol. 137, 189–203. https://doi.org/10.1016/S0031-0182(97)00109-0.

Wohlwend, S., Celestino, R., Reháková, D., Huck, S., Weissert, H., 2017. Late Jurassic to Cretaceous evolution of the eastern Tethyan Hawasina Basin (Oman Mountains). Sedimentology 64, 87–110. https://doi.org/10.1111/sed.12326.

Wright, P., Cherns, L., Hodges, P., 2003. Missing molluscs: field testing taphonomic loss in the Mesozoic through early large-scale aragonite dissolution. Geology 31, 211–214. https://doi.org/10.1130/0091-7613(2003)031<0211:MMFTTL>2.0.CO;2.

Yasuhara, M., Tittensor, D.P., Hillebrand, H., Worm, B., 2017. Combining marine macroecology and palaeoecology in understanding biodiversity: microfossils as a model. Biol. Rev. 92, 199–215. https://doi.org/10.1111/brv.12223.

Yobo, L.N., Brandon, A.D., Holmden, C., Lau, K.V., Eldrett, J., 2021. Changing inputs of continental and submarine weatheringsources of Sr to the oceans during OAE 2. Geochim. Cosmochim. Acta 303, 205–222. https://doi.org/10.1016/j.gca.2021.03.013.

Young, J.R., Davis, S.A., Bown, P.R., Mann, S., 1999. Coccolith ultrastructure and biomineralization. J. Struct. Biol. 126, 195–215. https://doi.org/10.1006/jsbi.1999.4132.

Young, J.R., Brown, P.R., Lees, J.A., 2021. Nannotax3 website. http://ina.tmsoc.org/nannotax3.

Zeebe, R.E., 2001. Seawater pH and isotopic paleotemperatures of Cretaceous oceans. Palaeogeogr., PalaeoclimatolPalaeoecol. 170, 49–57. https://doi.org/10.1016/S0031-0182(01)00226-7.

Zeebe, R.E., Tyrrell, T., 2018. Comment on "The effects of secular calcium and magnesium concentration changes on the thermodynamics of seawater acid/base chemistry: Implications for Eocene and Cretaceous ocean carbon chemistry and buffering" by Hain et al. (2015). Glob. Biogeochem. Cycles 32, 895–897.

Zeebe, R.E., Tyrrell, T., 2019. History of carbonate ion concentration over the last 100 million years II: revised calculations and new data. Geochim. Cosmochim. Acta 257, 373–392.

Zeebe, R.E., Westbroek, P., 2003. A simple model for the CaCO3 saturation state of the ocean: the "Strangelove", the "Neritan", and the "Cretan"Ocean. Geochem. Geophys. Geosyst. 4, 1104. https://doi.org/10.1029/2003GC000538.